UNIVERSITY OF BIRMINGHAM
University of Birmingham Research at Birmingham

# Characterization and activity test of commercial Ni/Al O , Cu/ZnO/Al O and prepared Ni-Cu/Al O catalysts for hydrogen production from methane and methanol fuels

Khzouz, M.; Bujalski, W.; Wood, J.; Pollet, B.

*DOI:*
10.1016/j.ijhydene.2012.07.026

*Document Version*
Early version, also known as pre-print

*Citation for published version (Harvard):*
Khzouz, M, Bujalski, W, Wood, J & Pollet, B 2012, 'Characterization and activity test of commercial Ni/Al O , Cu/ZnO/Al O and prepared Ni-Cu/Al O catalysts for hydrogen production from methane and methanol fuels', *International Journal of Hydrogen Energy*. https://doi.org/10.1016/j.ijhydene.2012.07.026

Link to publication on Research at Birmingham portal

**General rights**
Unless a licence is specified above, all rights (including copyright and moral rights) in this document are retained by the authors and/or the copyright holders. The express permission of the copyright holder must be obtained for any use of this material other than for purposes permitted by law.

•Users may freely distribute the URL that is used to identify this publication.
•Users may download and/or print one copy of the publication from the University of Birmingham research portal for the purpose of private study or non-commercial research.
•User may use extracts from the document in line with the concept of 'fair dealing' under the Copyright, Designs and Patents Act 1988 (?)
•Users may not further distribute the material nor use it for the purposes of commercial gain.

Where a licence is displayed above, please note the terms and conditions of the licence govern your use of this document.

When citing, please reference the published version.

**Take down policy**
While the University of Birmingham exercises care and attention in making items available there are rare occasions when an item has been uploaded in error or has been deemed to be commercially or otherwise sensitive.

If you believe that this is the case for this document, please contact UBIRA@lists.bham.ac.uk providing details and we will remove access to the work immediately and investigate.

Download date: 16. Apr. 2024

*Manuscript
Click here to view linked References

# Characterization and activity test of commercial $Ni/Al_2O_3$, $Cu/ZnO/Al_2O_3$ and prepared $Ni\text{-}Cu/Al_2O_3$ catalysts for hydrogen production from methane and methanol fuels

Martin Khzouz [*, 1], Joe Wood[2], Bruno Pollet[3] and Waldemar Bujalski[1]

[1] Centre for Hydrogen and Fuel Cell Research, School of Chemical Engineering

[2] Catalysts and Reactions Group, School of Chemical Engineering

The University of Birmingham, Edgbaston, B15 2TT, U.K

[3] HySA Systems Competence Centre , SAIAMC, University of the Western Cape, Private Bag X17,Modderdam Road, Bellville 7535, Cape Town, South Africa

*mnk932@bham.ac.uk; www.fuelcells.bham.ac.uk

**Abstract:**

In this study, methane and methanol steam reforming reactions over commercial $Ni/Al_2O_3$, commercial $Cu/ZnO/Al_2O_3$ and prepared $Ni\text{-}Cu/Al_2O_3$ catalysts were investigated. Methane and methanol steam reforming reactions catalysts were characterized using various techniques. The results of characterization showed that Cu particles increase the active particle size of Ni (19.3nm) in $Ni\text{-}Cu/Al_2O_3$ catalyst with respect to the commercial $Ni/Al_2O_3$ (17.9). On the other hand, Ni improves Cu dispersion in the same catalyst (1.74%) in comparison with commercial $Cu/ZnO/Al_2O_3$ (0.21%). A comprehensive comparison between these two fuels is established in terms of reaction conditions, fuel conversion, $H_2$ selectivity, $CO_2$ and CO selectivity. The prepared catalyst showed low selectivity for CO in both fuels and it was more selective to $H_2$, with $H_2$ selectivities of 99% in methane and 89% in methanol reforming reactions. A significant objective is to develop catalysts which can operate at lower temperatures and resist deactivation. Methanol steam reforming is carried out at a much lower temperature than methane steam reforming in prepared and commercial catalyst

(275-325°C). However, methane steam reforming can be carried out at a relatively low temperature on Ni-Cu catalyst (600-650°C) and at higher temperature in commercial methane reforming catalyst (700-800°C). Commercial $Ni/Al_2O_3$ catalyst resulted in high coke formation (28.3% loss in mass) compared to prepared $Ni\text{-}Cu/Al_2O_3$ (8.9%) and commercial $Cu/ZnO/Al_2O_3$ catalysts (3.5%).

**Keywords:** hydrogen; methane steam reforming**;** methanol steam reforming**;** fuel reformer; copper based catalyst; nickel based catalyst.

## 1 Introduction

About 700 billion $Nm^3$ of hydrogen is produced around the world and most of this hydrogen is produced on-site for industrial use [1]. The large and small scale production of hydrogen are likely to contribute to the energy market in the short to medium term in Europe [2]. However, the hydrogen produced at both scales requires an infrastructure network for storage, transmission and distribution, which is largely yet to be developed.

The hydrogen produced on-board in vehicles from its energy carriers can solve the technical problem of storing and distribution of hydrogen [3]. This can be achieved by using fuel processing technology. Hydrocarbons or alcohols are converted to pure hydrogen using a fuel reformer (fuel processor). Utilizing the hydrogen produced in proton exchange membrane fuel cell (PEMFC) to generate electricity could solve the future energy problems in transportation and domestic applications [4].

Steam reforming (equation 1) is widely used in industry to generate syngas ($H_2$ and CO) [5, 6]:

$$C_nH_mO_z + (n-z)H_2O \rightarrow nCO + (n-z+\frac{m}{2})H_2 \qquad \text{(eq. 1)}$$

Steam reforming is an endothermic reaction between the reactants (hydrocarbons and steam) which will need a significant amount of energy to activate the reaction. The reaction in the

fuel reformer depends on several factors; the temperature required for fuel reforming, the level of by products that the connected system can tolerate, the daily cycle of the reformer and the fuel used to produce hydrogen [7]. The choice of a suitable fuel reformer and fuel are the key aspects to the successful implementation of hydrogen fuel cell system [8]. A reformer integrated to a fuel cell is an attractive fuel source for the low temperature fuel cell such as PEMFC [9], which requires a high purity of hydrogen [10]. On the other hand, internal reforming in the fuel cell stack itself, could only be used with high temperature fuel cells such as solid oxide fuel cell (SOFC) and after taking into consideration a large amount of CO in the reformate stream [11, 12]. Table 1 shows the fuel that can be used for transportation and residential use applications [13].

Hydrogen can be extracted via methanol steam reforming. The endothermic methanol steam reforming reaction (equation 2) is the most frequently used method and it is possible to yield a gas product containing up to 75% hydrogen [14]. Although methanol has several disadvantages especially with regards to its distribution network [15], it is still a strong candidate fuel for fuel cell vehicles as the overall processing system would be simpler than other hydrocarbon fuels [16, 17]. In addition, methanol could be sold in single-use containers for use in portable fuel cell units for low power applications [15].

Methanol reforming process is carried out at a temperature range of 200-300 °C [6]. This kind of reaction employs copper based catalysts which usually consist of $Cu/ZnO/Al_2O_3$ [6]. The steam reforming of methanol (equation 2) would ideally produce hydrogen and carbon dioxide. However, this is not the case in the actual process, the reformate gases usually contain CO, $CO_2$, $H_2$, $H_2O$, $CH_3OH$ and other intermediate species produced via methanol decomposition reaction (equation 3) and water gas shift reaction (equation 4) [18-20].

$CH_3OH + H_2O \rightarrow CO_2 + 3H_2$ $\Delta H^\circ_{298} = +49.5$ kJ/mol (eq. 2)

$CH_3OH \rightarrow CO + 2H_2$ $\Delta H^\circ_{298} = +90.2$ kJ/mol (eq. 3)

$CO + H_2O \rightarrow CO_2 + H_2$ $\Delta H^\circ_{298} = -41$kJ/mol (eq. 4)

Steam reforming of methane (equation 5) produces hydrogen and carbon monoxide in a ratio of three to one. This main reaction is followed by a water gas shift process where carbon monoxide is converted into hydrogen and carbon dioxide as shown in (equation 4) [21]. The steam reforming of methane can be represented as the sum of steam reforming of methane and the water gas shift reaction as shown in (equation 6). The reaction is operated at high temperature (800 °C) over nickel-alumina based catalysts since high conversion of methane is achieved at this temperature [22]. A typical composition of reformed gas contains $H_2$, $CO_2$, unconverted methane and CO [23].

$CH_4 + H_2O \rightarrow CO + 3H_2$ $\Delta H^\circ_{298} = +206$kJ/mol (eq. 5)

$CH_4 + 2H_2O \rightarrow CO_2 + 4H_2$ $\Delta H^\circ_{298} = +165$kJ/mol (eq. 6)

Catalyst development is essential for designing an efficient, compact, fast start up and a low cost reformer [7]. Heterogeneous catalysts are majorly employed in steam reforming reactions so the reactants can readily pass through a solid catalyst bed [24]. These catalysts are categorized into three types: oxide catalysts, noble metal catalysts and base metal catalysts as illustrated in Table 2 [5]. A copper based catalyst is active at low temperature but its selectivity toward $H_2$ is low. In comparison with a copper based catalyst, a nickel based catalyst is highly selective toward $H_2$ at high temperature. However, it suffers from high coke formation and a severe deactivation.

In this work both methane and methanol steam reforming reactions on commercial $Ni/Al_2O_3$ and commercial $Cu/ZnO/Al_2O_3$ respectively have been studied. $Ni\text{-}Cu/Al_2O_3$ catalyst was prepared and tested for both reactions, with the aim to increase the catalytic

activity, lower the amount of carbon monoxide produced and develop a catalyst with a higher carbon tolerance. Ni-Cu catalysts have been previously studied for ethanol steam reforming [25-28], methane decomposition reaction [29-31], methane partial oxidation [32] and methanol steam reforming reactions [33]. It was reported in those studies that copper existence suppresses carbon formation. However, methanol and methane steam reforming reactions were not explored widely for such type of catalyst as well as compared to their commercial counterpart. Therefore, in the present study, a bimetallic catalyst which could show a high selectivity towards hydrogen and resist carbon deactivation in methane and methanol reforming compared with commercially available catalysts is investigated. The chemical and physical properties and catalytic performance are explored in this study. Catalyst characterization and activity tests are presented and comprehensive comparison for hydrogen generation via methane and methanol fuels are discussed.

## 2 Experimental

### 2.1 Catalyst

Two commercial reforming catalysts were selected to provide a basis for comparison with custom made catalysts. Copper based methanol reforming catalyst, HiFUEL R120 (Alfa Aesar) and nickel based steam reforming catalyst, HiFUEL R110 (Alfa Aesar) were characterised and tested for both methanol and methane steam reforming respectively. 5%Ni-5%Cu/$Al_2O_3$ catalysts were prepared using an impregnation method and the metal loadings in prepared catalyst were tested using X-ray fluorescence (XRF) Bruker S8 Tiger spectrometer type. Briefly, the metal solution (0.8M) of nickel nitrate ($Ni(NO_3)_2.6H_2O$) and copper nitrate ($Cu(NO_3)_2.3H_2O$) provided by Fisher Scientific were prepared using 13.8ml ethanol (Fisher scientific) with 99.8% purity. Six grams of $Al_2O_3$ (Johnson Matthey) trilobe-shaped catalyst supports were added to the solution and it was mixed for 2 hours using a Bandelin Sonorex

bath at 27°C. The catalyst was dried in a static oven overnight at 100°C, then the catalyst was heated for calcination to 500°C at a rate of 5°C/min, held at that temperature for five hours, then finally cooled at rate of 5°C/min to ambient temperature. The prepared catalyst was tested for both methanol and methane steam reforming reactions.

**2.2 Characterization**

The catalysts were characterized using scanning electron microscope (SEM), Brunauer Emmett Teller (BET) surface area test, CO chemisorption, X-ray diffraction (XRD), infrared (IR), and temperature programmed reduction (TPR) analyses.

SEM (Philips XL-30) of the catalyst was performed after coating with gold. BET surface area measurements [34] were performed using a Micrometrics ASAP 2010 analyser. Samples were measured using $N_2$ physisorption isotherms at -196°C. CO chemisorption tests were performed on a Micrometrics AutoChem 2920 Analyzer. Briefly, one gram of crushed catalyst was reduced using 10% $H_2$ in Argon at a flow rate 10 ml/min at 450°C for 2 hours. Helium gas was then introduced at a flow rate of 10 ml/min and the sample was cooled to ambient temperature. Finally, CO adsorption was investigated at a temperature of 30°C at a flow rate of 20 ml/min and helium as a carrier gas at a flow rate of 50 ml/min. Pulses of volume of 0.5389 ml (loop volume) were applied twenty times and any remaining CO which was not adsorbed on the catalyst was detected by a thermal conductivity detector (TCD) in the gas stream flowing from the tube outlet.

XRD was performed on a Bruker D8 Advance diffractometer using Cu Kα radiation (λ=0.154 nm). The data was recorded at room temperature in the two theta range from 5° to 90°. Infrared spectra for catalysts were recorded using a Bruker Tensor 37. The crushed catalyst was sieved with KBr at a particle size less than 75μm and 64 scans of absorbed spectra were monitored in the range 400$cm^{-1}$ to 4000$cm^{-1}$.

TPR experiments were investigated on one gram of sample using a Micrometrics AutoChem 2920 Analyzer. The sample was reduced at 500°C for one hour using 10% $H_2$ in Argon then the sample was cooled to ambient temperature. Finally, the temperature was increased to 900°C at 10°C/min and hydrogen uptake was recorded using a TCD.

**2.3 Activity test**

The multi fuel reformer experimental test rig was used to test the catalyst activity and selectivity for $H_2$, $CO_2$ and CO production. It consists of three modules; feeding module, reactor module and gas analysis module as shown in Fig. 1.

In methanol steam reforming, distilled water is mixed with pure methanol (99.99%) at a ratio of 1.7. The premix of methanol and water was injected to the reactor feed line using a Cole-Palmer EW-74930-05 series one pump to the vaporizer (110°C) at a constant flow rate of 0.06 ml/min. On the other hand, methane steam reforming was carried out by injecting pure methane (99.99%) into the reactor feed line at a flow rate of 25 ml/min and controlled by a Brooks mass flow controller. The steam generated as the water flowed through the trace heated section at temperature (110°C) is mixed with methane at ratio 3:1.

The reactor was constructed of stainless steel tube (316L) with inside diameter 15.6 mm and 395 mm length; the wall thickness of the pipe is 3.45 mm. The catalyst was packed in the reactor to a bed height of 26 mm for both reactions using a catalyst weight of 3 grams. The temperature inside the furnace was measured using K type thermocouple which is fixed at the center of the bed and the temperature of the furnace was controlled using a PID controller.

A gas chromatograph (Agilent 7890A) was used to detect hydrocarbons compounds, CO, $CO_2$ and $H_2$. The gas chromatograph was configured as a multi column instrument refinery gas analyzer. TCD2 back signal was used to detect methane, $CO_2$ and CO. The other

auxiliary TCD was used to detect hydrogen only. The flame ionization detector (FID) was used to measure multi hydrocarbon bonded compounds and any organic by products produced. The un-reacted water and methanol mixture were separated from the gaseous stream using a condenser. The condensation process was facilitated by ice cubes in a bath surrounding the pipe at a temperature of -2°C. The gas-liquid separator separates a gas stream from the un-reacted methanol mixture and water. The unconverted liquid reactants were analyzed using a Thermo Trace GC Ultra, which has a Thermo TR-5ms SQC column that detects water and methanol concentrations. A sample of 0.1µl was injected. The oven temperature of the GC was ramped from 35°C to 100° C at a rate of 5 °C/min and it was held at that temperature for 2 min.

The catalyst was reduced *in-situ* using pure hydrogen at a flow rate of 10ml/min. Both commercial $Ni/Al_2O_3$ and prepared $Ni\text{-}Cu/Al_2O_3$ were reduced at a temperature of 550°C and commercial $Cu/ZnO/Al_2O_3$ at 250°C. The temperature was raised at a rate of 5°C/min under an atmosphere of pure hydrogen at a flow rate of 10 ml/min. When the temperature of reduction was reached, hydrogen was injected for 30 minutes in the reduction procedure before switching to pure $N_2$ for purging purposes. Methanol steam reforming was carried out at temperatures (250, 275, 300, 325 °C) and methane steam reforming at temperatures (500, 550, 600, 650, 700 °C) in order to find the optimum operating conditions. The warm up period for reaction was one hour. After that, reformates were sampled every 15 minutes for three hours of operation.

## 3. Results and discussion

### 3.1 SEM test

Fig. 2 shows SEM images for tested catalysts at 90µm scale. The images show the textural distribution of metals on support on micro scale. It is clear from Fig. 2(a-c) that each

catalyst has its own metal clusters on the support with various sizes [35].

### 3.2 BET and CO chemisorptions tests

Table 3 summarizes the physical characteristics of catalysts. The prepared Ni-Cu/$Al_2O_3$ catalysts showed high surface areas and pore volumes compared to commercial catalysts. Low pore volume in commercial Ni/$Al_2O_3$ catalysts can be interpreted as being due to high metal loading through which Ni particles might block pores of $Al_2O_3$ during metal deposition [32, 33]. The CO chemisorption experiment revealed that Ni-Cu/$Al_2O_3$ catalyst has a higher metallic surface area and metal dispersion than commercial Cu/ZnO/$Al_2O_3$ and Ni/$Al_2O_3$ catalysts. De Rogatis et al [32] had prepared Ni-Cu/$Al_2O_3$ catalyst which showed a BET surface area of 82 $m^2$/g. On the other hand, the commercial catalyst of Ni/$Al_2O_3$ studied by Hou and Hughes [36] resulted in a BET surface area of 14.30 $m^2$/g, which is slightly higher than commercial catalyst tested in the present study (12 $m^2$/g). The commercial Cu/Zno/$Al_2O_3$ catalyst studied by Jones and Hagelin [37] showed a BET surface area of 68$m^2$/g [37]. Ginés et al [38] had studied the metallic copper dispersion and it was observed that the copper dispersion varied between a minimum value of 0.5% and a maximum value of 5%. This was interpretd to the amount of hydrotalcite contained in the hydroxycarbonate precursor, the higher the hydrotalcite content leads to the higher the copper metal dispersion in the resulting catalyst.

In this study, a lower value of dispersion (0.21%) was observed due two main resons, namely; the large particle size of copper and the conventional preperation method (co-precipitation) used [39-42]. The value of dispersion reported here (1.29%) for commercial Ni/$Al_2O_3$ catalyst is similar to one reported by Oliveira et al [43] (1.42%) and by Seo et al [44] (1.5%). Prepared Ni-Cu/$Al_2O_3$ catalyst showed a metal dispersion slightly higher than commercial Ni catalyst. However, prepared catalyst in this study had low metallic dispersion

(1.74%) compared to the prepared catalyst (4.1%) studied by De Rogatis et al [33]. This can be related to the large particle size of present catalyst and several treatment conditions during impregnation method such; calicination temperature and type of the support used [38].

### 3.3 XRD test

XRD test from 5° to 90° in Fig. 3 shows the characteristics peaks of metal oxides of the catalyst. In this test the XRD patterns of the alumina catalyst support show the presence of $\gamma$-$Al_2O_3$ and traces of $\theta$-$Al_2O_3$. In order to calculate the average particle diameter of metal oxides, Scherrer's equation, $t = \frac{0.9\lambda}{B\cos\theta}$, is applied. The average particle diameter of NiO is 17.9 nm in $Ni/Al_2O_3$ catalyst and CuO is 17.4 nm in $Cu/ZnO/Al_2O_3$ catalyst. XRD patterns of Ni-$Cu/Al_2O_3$ proved the formation of $Ni_xCu_{1-x}$ O and a shift in peaks compared to commercial catalyst are present. The average particle crystallite diameter of prepared catalyst is 19.3 nm. This can be related to more crystallites in the particles of Ni or Cu with respect to the commercial catalyst.

### 3.4 IR test

Fig. 4 shows the infrared spectra for the prepared and commercial catalysts. Applying infrared spectra for catalysts showed high and low wavenumber regions. At low wavenumber regions, Ni-$Cu/Al_2O_3$ catalyst showed three active peaks, of which two might result from pure Ni (1375 $cm^{-1}$) and Cu particles (1502 $cm^{-1}$), in addition a third peak for an alloy of Ni-Cu particles (1643 $cm^{-1}$) as shown in Fig. 4. High wavenumber region (3386 $cm^{-1}$) could be related to Ni surface spinel [45]. Band positions are affected by various variables such as temperature, surface concentrations, and the presence of other adsorbed species [45, 46]. Therefore, the prepared catalyst showed shift in peaks compared to the commercial catalysts which is explained later in TPR test. At least three different oxide phases were detected in the spectra for the Ni commercial system: $Al_2O_3$, NiO and the so-called nickel surface spinel

appeared in infrared test as reported by Ryczkowski [45]. The peaks were located at wavenumbers of 1028cm$^{-1}$, 1444 cm$^{-1}$ and 3386 cm$^{-1}$ respectively. The commercial copper spectra displayed a band at 1515 cm$^{-1}$ (CuO) and 3311 cm$^{-1}$ (ZnO) which agree with the Edwards and Schrader study [46].

**3.5 TPR test**

Hydrogen uptakes (Fig. 5) for Cu/ZnO/$Al_2O_3$ catalyst showed one peak at 255°C. The TPR trace for Ni/$Al_2O_3$ catalyst displayed two peaks at 670°C and 776°C, which were interpreted as weak and strong interactions between NiO and the $Al_2O_3$ support respectively [32, 47, 48]. Three hydrogen uptake peaks were displayed on prepared Ni-Cu/$Al_2O_3$ catalyst. The first peak at 180°C is related to interactions between the CuO and $Al_2O_3$ support. The next broad peak at 390°C is associated with Ni-Cu alloy particles and the last peak at 620°C might be due to NiO reduction. TPR data obtained from commercial copper catalyst was totally agree with TPR test carried out (250°C) by Samuel and Hagelin [37]. Two reduction bands displayed by Ni catalyst are associated firstly with the reduction of nickel oxide interacting with alumina and secondly a high reduction band is attributed to the reduction of nickel aluminate phase [44]. TPR profiles of supported nickel catalysts are strongly affected by the nature of metal-support interaction [49]. NiO species supported on $Al_2O_3$ are reduced at around 500–700 °C and the reduction of nickel aluminate occurs at higher temperature above 800°C because of the strong interaction between nickel species and alumina [50]. Ni-Cu catalyst supported on $Al_2O_3$ prepared by De Rogatis et al [32]agrees with the TPR test reported in this work and showed three TPR peaks. In their study, the first reduction peak appeared at about 160°C and was associated with the reduction of CuO. The second peak at 390°C which was attributed to the reduction of Ni-based species promoted by the presence of metallic Cu as mentioned by Lee et al [51]. The third peak at about 770 °C was related to strong interaction of Ni oxides species with the $Al_2O_3$. The difference in the position of

reduction peaks reported in this work (Fig. 5) is related to the fact that reduction peaks strongly depends on the particle dimension and the interaction strength between metal particles and the support.

### 3.6 Activity test

$H_2$ selectivity (equation 7), fuel conversion (equation 8 and 9), $CO_2$ and CO selectivity (equation 10 and 11) were investigated for both fuels and catalysts. These were calculated from the following equations:

$$H_2 \text{ selectivity} = \frac{[H_2]}{[H_2]+[CO_2]+[CO]}.100 \qquad \text{(eq. 7)}$$

$$\text{Methanol conversion} = \frac{CH_3OH_{in} - CH_3OH_{out}}{CH_3OH_{in}}.100 \qquad \text{(eq. 8)}$$

$$\text{Methane conversion} = \frac{CH_{4\,in} - CH_{4\,out}}{CH_{4\,in}}.100 \qquad \text{(eq. 9)}$$

$$CO_2 \text{ selectivity} = \frac{[CO_2]}{[CO_2]+[H_2]+[CO]}.100 \qquad \text{(eq. 10)}$$

$$CO \text{ selectivity} = \frac{[CO]}{[CO]+[H_2]+[CO_2]}.100 \qquad \text{(eq. 11)}$$

Fig. 6 shows methanol steam reforming over commercial $Cu/ZnO/Al_2O_3$ catalyst. Methanol conversion was 99% and hydrogen selectivity was 86% at 325°C. With increasing temperature from 250°C to 325°C, the catalyst selectivity towards CO increased and $CO_2$ decreased. Investigating methanol steam reforming using prepared $Ni\text{-}Cu/Al_2O_3$ as presented in Fig. 7 resulted in 99% methanol conversion and hydrogen selectivity was 89% at 275°C. In contrast to commercial methanol steam reforming catalyst, $Ni\text{-}Cu/Al_2O_3$ catalyst selectivity toward CO with increased temperature decreased and $CO_2$ selectivity increased as can be observed from the data shown in Table 4.

Methanol steam reforming could be assumed to be the sequence of methanol decomposition reaction (equation 3) followed by water gas shift reaction (equation 4) [18]. As a result, Pepply et al [19] proposed two active sites on copper based catalyst. One site is responsible of steam reforming reaction and water gas shift reaction while the second site activates the decomposition reaction. The increase on CO selectivity over commercial $Cu/ZnO/Al_2O_3$ with increasing the temperature is related to high active reverse water gas shift reaction. However, this is not the case on prepared $Ni\text{-}Cu/Al_2O_3$ catalyst. The low selectivity towards CO suggests that water gas shift reaction is the dominant reaction at high temperature which can be related to fact that Cu doesn't easily dissociate CO [52] which leads to decrease on $CO/CO_2$ hydrogenation activity of Ni catalyst [33].

Methane steam reforming reaction over commercial $Ni/Al_2O_3$ catalyst showed 89% methane fuel conversion and 96% for hydrogen selectivity at 700°C (Fig. 8). The catalyst selectivity for CO with increasing temperature increased and $CO_2$ selectivity decreased as presented in Fig. 8. The same reaction (Fig. 9) was applied on prepared $Ni\text{-}Cu/Al_2O_3$ catalyst and 89% of methane fuel conversion was achieved at 650°C with 99% hydrogen selectivity at the same temperature. Increasing the temperature, the prepared $Ni\text{-}Cu/Al_2O_3$ catalyst

displayed a lower selectivity for CO and $CO_2$ in comparison with commercial $Ni/Al_2O_3$ catalyst as illustrated in Table 5.

Methane steam reforming is represented by three predominant reactions (equation 4-6 ) [53]. Since methane steam reforming is very endothermic, the reaction temperature will significantly affect the equilibrium compositions of the product as well as the conversion [54]. Increasing the temperature (500-700 °C) both commercial $Ni/Al_2O_3$ and prepared $Ni-Cu/Al_2O_3$ catalysts showed an increase in fuel conversion. However, prepared $Ni-Cu/Al_2O_3$ showed a low selectivity towards CO and $CO_2$ than commercial $Ni/Al_2O_3$ catalyst. This can be related to fact that Ni-Cu alloy could be responsible for the blocking and decrease of the sites involved in the carbon growth [31] as explained in Boudouard reaction (equation 12) [55]. Therefore, the Cu addition suppresses the carbon deposition and act as stabilizing agent in $Ni-Cu/Al_2O_3$ catalyst [32, 51].

$$2CO \rightarrow C + CO_2 \qquad \text{(eq. 12)}$$

Fig. 10 presents optimal steam reforming results in both fuels and all catalysts tested based on CO selectivity. Methanol reforming catalyst was less selective for CO than commercial methane reforming catalyst. The prepared catalyst was less selective for CO in comparison with both commercial Ni and Cu based catalysts. In addition, methane steam reforming can be carried out at lower temperature on Ni-Cu catalyst (650°C). However, reaction over commercial methane reforming catalyst is carried out at 700°C. The low temperature of conversion is important for system material selection as well as requiring less external heating and insulation, all of which can lead to a smaller, more efficient integrated fuel cell reformer system [15]. As well as the low levels of CO formation on active catalyst will reduce the size of CO cleaning unit which can demonstrate compact fuel reformer for portable and onboard applications [56].

Thermo gravimetric analysis (TGA) was carried out for used catalysts at high and low temperature. The commercial $Ni/Al_2O_3$ catalyst resulted in high coke formation (28.3%) compared to prepared $Ni\text{-}Cu/Al_2O_3$ (8.9 %) and commercial $Cu/ZnO/Al_2O_3$ (3.5%) catalysts as shown in Fig. 11 and illustrated in Table 6. It is known that deactivation of Ni based catalysts can be due to carbon formation during reaction [57, 58]. This was clearly suppressed by copper addition in $Ni\text{-}Cu/Al_2O_3$ catalyst [51].

De Rogatis et al [33] studied the catalytic performance of the bimetallic system of $Ni\text{-}Cu/Al_2O_3$. They found that methanol conversion starts above 150°C and the complete conversion is reached around 205°C. $CO_2$ and CO product distributions follow opposite trends at temperatures below 300°C, which strongly agrees with the results presented here. In the same study, no significant deactivation of catalyst activity and carbon formation was observed as proven by the TGA test reported here. Huang et al [59] used a copper commercial catalyst as a reference in their study. The commercial catalyst showed 70% methanol conversion at a temperature of 300°C. This can be related to the composition of catalyst and the low steam to methanol ratio applied. Matsumura and Ishibe [60] also used commercial copper catalyst as a reference. They reported 1.1 % selectivity of CO and 59% of methanol conversion at a temperature of 300°C and low steam to methanol ratio. Seo et al [54] mentioned in their thermal energy analysis study the favourable operating conditions for steam reforming of methane. They achieved 99% methane conversion at a steam to carbon ratio of 1.9 and reactor temperature of 800°C. The commercial nickel catalyst here showed a similar trend for fuel conversion and gaseous selectivity and strongly confirmed the gas product composition published by Heinzel et al [23]. Both methane tested catalysts showed better hydrogen selectivity and methane conversion trends at temperatures above 600°C with lower selectivity for CO than previous thermodynamic studies [21, 54, 61]. To the best of the author's knowledge, it was difficult to find a literature study that had tested $Ni\text{-}Cu/Al_2O_3$ on

methane steam reforming [62]. However; the study carried by Huang and Jhao [63] proved that Ni-Cu interaction enhances the activity of steam reforming of methane and decreases the CO production rate as shown in the activity test reported here.

## 4 Conclusions

The results of characterization showed that the prepared Ni-Cu/$Al_2O_3$ catalyst is reduced at 390°C. Various types of metal interactions with the support are present in the TPR test. In Ni-Cu/$Al_2O_3$ catalyst, Cu particles increase the active particle size of Ni (19.3nm) in Ni-Cu/$Al_2O_3$ catalyst with respect to the commercial Ni/$Al_2O_3$ (17.9 nm). On the other hand, Ni improves Cu dispersion in the same catalyst (1.74%) in comparison with commercial Cu/ZnO/$Al_2O_3$ (0.21%). Ni-Cu/$Al_2O_3$ showed a high BET surface area compared to the commercial catalysts. XRD patterns of Ni-Cu/$Al_2O_3$ proved the formation of $Ni_xCu_{1-x}$ O and there is a shift of peaks compared to commercial catalyst. IR test at low frequency showed three peaks in Ni-Cu/$Al_2O_3$ which are related to pure Ni and Cu metal plus an alloy of Ni-Cu particles.

A comprehensive comparison between two fuels is established in term of reaction conditions, fuel conversion, $H_2$ selectivity, $CO_2$ selectivity and CO selectivity. The prepared catalyst showed lower selectivity for CO in both fuels and Ni-Cu catalyst was more selective to $H_2$ compared to commercial catalysts. Methanol steam reforming over commercial Cu/ZnO/$Al_2O_3$ catalyst showed 99% fuel conversion and hydrogen selectivity was 86% at 325°C. Ni-Cu/$Al_2O_3$ resulted in 99% methanol conversion and hydrogen selectivity was 89% at 275°C. Investigating methane steam reforming reaction over commercial Ni/$Al_2O_3$ catalyst showed 89% methane fuel conversion and 96% for hydrogen selectivity at 700°C. The prepared Ni-Cu/$Al_2O_3$ catalyst achieved 89% of methane fuel conversion and 99% hydrogen selectivity at 650°C. Methanol steam reforming is carried out at a much lower temperature

(275-325°C) than needed in methane reforming. However, methane steam reforming can be carried out at a relatively low temperature on Ni-Cu catalyst (600-650°C) and at higher temperature in commercial methane reforming catalyst (700-800°C). TGA test showed that commercial $Ni/Al_2O_3$ catalyst resulted in high coke formation (28.3% loss in mass) compared to prepared $Ni-Cu/Al_2O_3$ (8.9%) and commercial $Cu/ZnO/Al_2O_3$ catalysts (3.5%). This can be related to fact that Ni-Cu alloy is responsible for the blocking and decrease of the sites involved in the carbon growth during methane steam reforming reaction. Therefore, the Cu addition suppresses the carbon deposition and acts as stabilizing agent in $Ni-Cu/Al_2O_3$ during steam reforming reaction.

**Acknowledgements**

Centre for Applied Energy Research (CAER-int, Jordan) is acknowledged for the financial support.

**References**

[1] Ball M, Wietschel M. The future of hydrogen - opportunities and challenges. International Journal of Hydrogen Energy. 2009;34:615-27.
[2] Mueller-Langer F, Tzimas E, Kaltschmitt M, Peteves S. Techno-economic assessment of hydrogen production processes for the hydrogen economy for the short and medium term. International Journal of Hydrogen Energy. 2007;32:3797-810.
[3] Budzianowski WM. Value-added carbon management technologies for low CO2 intensive carbon-based energy vectors. Energy. 2012;41:280-97.
[4] Larminie J, Dicks A. Fuel Cell Systems Explained. 2 ed: Wiley; 2003.
[5] Xuan J, Leung MKH, Leung DYC, Ni M. A review of biomass-derived fuel processors for fuel cell systems. Renewable and Sustainable Energy Reviews. 2009;13:1301-13.
[6] Kolb G. Fuel Processing For Fuel Cells. Weinheim: Wiley-VCH; 2008.
[7] Ahmed S, Kumar R, Krumpelt M. Fuel processing for fuel cell power systems. Fuel Cells Bulletin. 1999;2:4-7.
[8] Cipitì F, Pino L, Vita A, Laganà M, Recupero V. Performance of a 5 kWe fuel processor for polymer electrolyte fuel cells. International Journal of Hydrogen Energy. 2008;33:3197-203.
[9] Faur Ghenciu A. Review of fuel processing catalysts for hydrogen production in PEM fuel cell systems. Current Opinion in Solid State and Materials Science. 2002;6:389-99.
[10] Budzianowski WM. An oxy-fuel mass-recirculating process for H2 production with CO2 capture by autothermal catalytic oxyforming of methane. International Journal of Hydrogen Energy. 2010;35:7454-69.
[11] Clarke SH, Dicks AL, Pointon K, Smith TA, Swann A. Catalytic aspects of the steam reforming of hydrocarbons in internal reforming fuel cells. Catalysis Today. 1997;38:411-23.
[12] Qi A, Peppley B, Karan K. Integrated fuel processors for fuel cell application: A review. Fuel Processing Technology. 2007;88:3-22.
[13] F. Brown L. A comparative study of fuels for on-board hydrogen production for fuel-cell-powered automobiles. International Journal of Hydrogen Energy. 2001;26:381-97.
[14] Lindström B, Pettersson LJ. Development of a methanol fuelled reformer for fuel cell applications. Journal of Power Sources. 2003;118:71-8.

[15] Palo DR, Dagle RA, Holladay JD. Methanol Steam Reforming for Hydrogen Production. Chemical Reviews. 2007;107:3992-4021.
[16] McNicol BD, Rand DAJ, Williams KR. Fuel cells for road transportation purposes — yes or no? Journal of Power Sources. 2001;100:47-59.
[17] Joensen F, Rostrup-Nielsen JR. Conversion of hydrocarbons and alcohols for fuel cells. Journal of Power Sources. 2002;105:195-201.
[18] Peppley BA, Amphlett JC, Kearns LM, Mann RF. Methanol–steam reforming on Cu/ZnO/Al2O3. Part 1: the reaction network. Applied Catalysis A: General. 1999;179:21-9.
[19] Peppley BA, Amphlett JC, Kearns LM, Mann RF. Methanol–steam reforming on Cu/ZnO/Al2O3 catalysts. Part 2. A comprehensive kinetic model. Applied Catalysis A: General. 1999;179:31-49.
[20] Lwin Y, Daud WRW, Mohamad AB, Yaakob Z. Hydrogen production from steam-methanol reforming: thermodynamic analysis. International Journal of Hydrogen Energy. 2000;25:47-53.
[21] Ávila-Neto CN, Dantas SC, Silva FA, Franco TV, Romanielo LL, Hori CE, et al. Hydrogen production from methane reforming: Thermodynamic assessment and autothermal reactor design. Journal of Natural Gas Science and Engineering. 2009;1:205-15.
[22] Matsumura Y, Nakamori T. Steam reforming of methane over nickel catalysts at low reaction temperature. Applied Catalysis A: General. 2004;258:107-14.
[23] Heinzel A, Vogel B, Hübner P. Reforming of natural gas—hydrogen generation for small scale stationary fuel cell systems. Journal of Power Sources. 2002;105:202-7.
[24] Richardson JT. Principles of Catalyst Development. New York: Plenum press; 1989.
[25] De Rogatis L, Montini T, Lorenzut B, Fornasiero P. NiCu/Al2O3 based catalysts for hydrogen production. Energy & Environmental Science. 2008;1:501-9.
[26] Carrero A, Calles JA, Vizcaíno AJ. Hydrogen production by ethanol steam reforming over Cu-Ni/SBA-15 supported catalysts prepared by direct synthesis and impregnation. Applied Catalysis A: General. 2007;327:82-94.
[27] Vizcaíno AJ, Carrero A, Calles JA. Hydrogen production by ethanol steam reforming over Cu–Ni supported catalysts. International Journal of Hydrogen Energy. 2007;32:1450-61.
[28] Mariño F, Boveri M, Baronetti G, Laborde M. Hydrogen production from steam reforming of bioethanol using Cu/Ni/K/γ-Al2O3 catalysts. Effect of Ni. International Journal of Hydrogen Energy. 2001;26:665-8.
[29] Echegoyen Y, Suelves I, Lázaro MJ, Moliner R, Palacios JM. Hydrogen production by thermocatalytic decomposition of methane over Ni-Al and Ni-Cu-Al catalysts: Effect of calcination temperature. Journal of Power Sources. 2007;169:150-7.
[30] Chen J, Li Y, Li Z, Zhang X. Production of COx-free hydrogen and nanocarbon by direct decomposition of undiluted methane on Ni-Cu-alumina catalysts. Applied Catalysis A: General. 2004;269:179-86.
[31] Reshetenko TV, Avdeeva LB, Ismagilov ZR, Chuvilin AL, Ushakov VA. Carbon capacious Ni-Cu-Al2O3 catalysts for high-temperature methane decomposition. Applied Catalysis A: General. 2003;247:51-63.
[32] De Rogatis L, Montini T, Cognigni A, Olivi L, Fornasiero P. Methane partial oxidation on NiCu-based catalysts. Catalysis Today. 2009;145:176-85.
[33] De Rogatis L, Montini T, Lorenzut B, Fornasiero P. NixCuy/Al2O3 based catalysts for hydrogen production. Energy & Environmental Science. 2008;1:501-9.
[34] Brunauer S, P.H.Emmett, Teller E. Adsorption of Gases in Multimolecular Layers. CONTRIBUTION FROM THE BUREAU OF CHEMISTRY AND SOILS AND GEORGE WASHINGTON UNIVERSITIY. 1938.
[35] Oliveira ELG, Grande CA, Rodrigues AE. Steam methane reforming in a Ni/Al2O3 catalyst: Kinetics and diffusional limitations in extrudates. The Canadian Journal of Chemical Engineering. 2009;87:945-56.
[36] Hou K, Hughes R. The kinetics of methane steam reforming over a Ni/α-Al2O catalyst. Chemical Engineering Journal. 2001;82:311-28.
[37] Jones SD, Hagelin-Weaver HE. Steam reforming of methanol over CeO2- and ZrO2-promoted Cu-ZnO catalysts supported on nanoparticle Al2O3. Applied Catalysis B: Environmental. 2009;90:195-204.
[38] Ginés MJL, Amadeo N, Laborde M, Apesteguía CR. Activity and structure-sensitivity of the water-gas shift reaction over CuZnAl mixed oxide catalysts. Applied Catalysis A: General. 1995;131:283-96.
[39] Yao C-Z, Wang L-C, Liu Y-M, Wu G-S, Cao Y, Dai W-L, et al. Effect of preparation method on the hydrogen production from methanol steam reforming over binary Cu/ZrO2 catalysts. Applied Catalysis A: General. 2006;297:151-8.
[40] Shishido T, Yamamoto Y, Morioka H, Takaki K, Takehira K. Active Cu/ZnO and Cu/ZnO/Al2O3 catalysts prepared by homogeneous precipitation method in steam reforming of methanol. Applied Catalysis A: General. 2004;263:249-53.
[41] Shishido T, Yamamoto Y, Morioka H, Takehira K. Production of hydrogen from methanol over Cu/ZnO and Cu/ZnO/Al2O3 catalysts prepared by homogeneous precipitation: Steam reforming and oxidative steam reforming. Journal of Molecular Catalysis A: Chemical. 2007;268:185-94.
[42] Águila G, Jiménez J, Guerrero S, Gracia F, Chornik B, Quinteros S, et al. A novel method for preparing

high surface area copper zirconia catalysts: Influence of the preparation variables. Applied Catalysis A: General. 2009;360:98-105.
[43] Oliveira ELG, Grande CA, Rodrigues AE. Methane steam reforming in large pore catalyst. Chemical Engineering Science. 2010;65:1539-50.
[44] Seo JG, Youn MH, Jung JC, Song IK. Effect of preparation method of mesoporous Ni–Al2O3 catalysts on their catalytic activity for hydrogen production by steam reforming of liquefied natural gas (LNG). International Journal of Hydrogen Energy. 2009;34:5409-16.
[45] Janusz R. IR spectroscopy in catalysis. Catalysis Today. 2001;68:263-381.
[46] Edwards JF, Schrader GL. Infrared spectroscopy of copper/zinc oxide catalysts for the water-gas shift reaction and methanol synthesis. The Journal of Physical Chemistry. 1984;88:5620-4.
[47] Roh H-S, Jun K-W, Dong W-S, Chang J-S, Park S-E, Joe Y-I. Highly active and stable Ni/Ce–ZrO2 catalyst for H2 production from methane. Journal of Molecular Catalysis A: Chemical. 2002;181:137-42.
[48] Ye J, Li Z, Duan H, Liu Y. Lanthanum Modified Ni/γ-Al2O3 Catalysts for Partial Oxidation of Methane. Journal of Rare Earths. 2006;24:302-8.
[49] Seo JG, Youn MH, Park S, Song IK. Effect of calcination temperature of mesoporous alumina xerogel (AX) supports on hydrogen production by steam reforming of liquefied natural gas (LNG) over Ni/AX catalysts. International Journal of Hydrogen Energy. 2008;33:7427-34.
[50] Youn MH, Seo JG, Kim P, Song IK. Role and effect of molybdenum on the performance of Ni-Mo/γ-Al2O3 catalysts in the hydrogen production by auto-thermal reforming of ethanol. Journal of Molecular Catalysis A: Chemical. 2007;261:276-81.
[51] Lee J-H, Lee E-G, Joo O-S, Jung K-D. Stabilization of Ni/Al2O3 catalyst by Cu addition for CO2 reforming of methane. Applied Catalysis A: General. 2004;269:1-6.
[52] Ponec V. Chapter 4 Selectivity in The Syngas Reactions: The Role of Supports and Promoters in The Activation of Co and In The Stabilization of Intermediates. In: Guczi L, editor. Studies in Surface Science and Catalysis: Elsevier; 1991. p. 117-57.
[53] Xu J, Froment GF. Methane steam reforming, methanation and water-gas shift: I. Intrinsic kinetics. AIChE Journal. 1989;35:88-96.
[54] Seo YS, Shirley A, Kolaczkowski ST. Evaluation of thermodynamically favourable operating conditions for production of hydrogen in three different reforming technologies. Journal of Power Sources. 2002;108:213-25.
[55] Freni S, Calogero G, Cavallaro S. Hydrogen production from methane through catalytic partial oxidation reactions. Journal of Power Sources. 2000;87:28-38.
[56] Arzamendi G, Diéguez PM, Montes M, Centeno MA, Odriozola JA, Gandía LM. Integration of methanol steam reforming and combustion in a microchannel reactor for H2 production: A CFD simulation study. Catalysis Today. 2009;143:25-31.
[57] Miao Q, Xiong G, Sheng S, Cui W, Xu L, Guo X. Partial oxidation of methane to syngas over nickel-based catalysts modified by alkali metal oxide and rare earth metal oxide. Applied Catalysis A: General. 1997;154:17-27.
[58] Sperle T, Chen D, Lødeng R, Holmen A. Pre-reforming of natural gas on a Ni catalyst: Criteria for carbon free operation. Applied Catalysis A: General. 2005;282:195-204.
[59] Huang G, Liaw B-J, Jhang C-J, Chen Y-Z. Steam reforming of methanol over CuO/ZnO/CeO2/ZrO2/Al2O3 catalysts. Applied Catalysis A: General. 2009;358:7-12.
[60] Matsumura Y, Ishibe H. Suppression of CO by-production in steam reforming of methanol by addition of zinc oxide to silica-supported copper catalyst. Journal of Catalysis. 2009;268:282-9.
[61] Balasubramanian B, Lopez Ortiz A, Kaytakoglu S, Harrison DP. Hydrogen from methane in a single-step process. Chemical Engineering Science. 1999;54:3543-52.
[62] Khzouz M, Wood J, Kendall K, Bujalski W. Characterization of Ni–Cu-based catalysts for multi-fuel steam reformer. International Journal of Low-Carbon Technologies. 2011.
[63] Huang T-J, Jhao S-Y. Ni-Cu/samaria-doped ceria catalysts for steam reforming of methane in the presence of carbon dioxide. Applied Catalysis A: General. 2006;302:325-32.

**Abbreviations**

PEMFC Proton Exchange Membrane Fuel cell

SOFC Solid Oxide Fuel Cell

SEM Scanning electron microscope

BET Brunauer Emmett Teller

XRD X-ray diffraction

IR Infrared

TPR Temperature programmed reduction

TCD Thermal conductivity detector

TGA Thermo gravimetric analysis

GC Gas chromatograph

XRF X-ray fluorescence

FID Flame Ionization Detector

**Table captions**

Table 1. Characteristics of steam reforming process for producing hydrogen via intermediate fuels [13].

Table 2. Summary of the advantages and disadvantages of reforming catalysts from the literature [5].

Table 3. Physical characteristics of tested catalysts.

Table 4. Gas feed composition for methanol steam reforming at various operating conditions.

Table 5. Gas feed composition for methane steam reforming at various operating conditions.

Table 6. Percentage of mass change of commercial and prepared catalysts at various operating conditions.

**Figure captions**

Figure 1. Multi fuel reformer experimental test rig.

Figure 2. SEM of (a) $Cu/ZnO/Al_2O_3$ (b) $Ni/Al_2O_3$ (c) $Ni\text{-}Cu/Al_2O_3$.

Figure 3. XRD diffraction patterns for commercial and prepared catalysts.

Figure 4. Infrared spectra for commercial and prepared catalysts.

Figure 5. TPR of commercial and prepared catalysts.

Figure 6. Methanol steam reforming over $Cu/ZnO/Al_2O_3$ catalyst.

Figure 7. Methanol steam reforming over $Ni\text{-}Cu/Al_2O_3$ catalyst.

Figure 8. Methane steam reforming over $Ni/Al_2O_3$ catalyst.

Figure 9. Methane steam reforming over $Ni\text{-}Cu/Al_2O_3$ catalyst.

Figure 10. Optimal reforming results for both fuels and catalysts tested.

Figure 11. TGA of commercial and prepared catalysts.

Table 1. Characteristics of steam reforming process for producing hydrogen via intermediate fuels [13].

| Steam Reforming of | CO in Product (mol%) initial reaction | Temperature range of initial reaction (°C) | Total theoretical input energy to process (kJ/kg of usable $H_2$ ) |
|---|---|---|---|
| Methane | 11.2 | 727-827 | 0.141 |
| Methanol | 0.8 | 227-287 | 0.145 |
| Ethanol | 10-14 | ~527-727 | 0.144 |
| Gasoline, diesel fuel and aviation jet fuel | 20 | 727-877 | 0.148 |

Table 2. Summary of the advantages and disadvantages of reforming catalysts from the literature [5].

| Category | Example | Properties |
|---|---|---|
| Oxide catalysts | MgO, $Al_2O_3$, $V_2O_5$, ZnO, $TiO_2$, $La_2O_3$, $CeO_2$, $La_2O_3$–$Al_2O_3$, $CeO_2$–$Al_2O_3$, MgO–$Al_2O_3$ $Al_2O_3$ and $V_2O_5$ | Normally good activity but low selectivity. |
| Noble metal catalysts | Rh, Ru, Pt and Pd | Active, high selectivity but the cost is high. |
| Base metal catalysts | Co-based (Co/ZnO), Cu-based and Ni-based ($Ni/Al_2O_3$) | Co-based: good catalytic performance, but rapidly deactivate.<br><br>Cu-based: good activity at low reaction temperature, while $H_2$ selectivity is poor.<br><br>Ni-based: high conversion and the $H_2$ selectivity, but may occur coke deposition and a severe deactivation. |

Table 3. Physical characteristics of tested catalysts.

| Characteristics | $Cu/ZnO/Al_2O_3$ (Commercial) | $Ni/Al_2O_3$ (Commercial) | $Ni\text{-}Cu/Al_2O_3$ (prepared) |
|---|---|---|---|
| Composition [a] | Cu=50% | Ni=40% | Ni=5% |
| | ZnO=25% | $Al_2O_3$=60% | Cu=5% |
| | $Al_2O_3$=25% | | $Al_2O_3$=90% |
| Nitrogen BET area ($m^2/g$) | 74 | 12 | 93 |
| Pore volume (ml/g) | 0.22 | 0.06 | 0.45 |
| Active metal area ($m^2/g$) | 1.32 | 8.62 | 11.38 |
| Dispersion | 0.21% | 1.29% | 1.74% |
| Crystallite size Å | 119 | 187 | 193 |

[a] As provided from manufacturer data sheets or tested by XRF for prepared catalyst.

Table 4. Gas feed composition for methanol steam reforming at various operating conditions.

| Temperature (°C) | $H_2$ Selectivity $Cu/ZnO/Al_2O_3$ | $H_2$ Selectivity Ni-$Cu/Al_2O_3$ | $CO_2$ Selectivity $Cu/ZnO/Al_2O_3$ | $CO_2$ Selectivity Ni-$Cu/Al_2O_3$ | CO Selectivity $Cu/ZnO/Al_2O_3$ | CO Selectivity Ni-$Cu/Al_2O_3$ | Conversion $Cu/ZnO/Al_2O_3$ | Conversion Ni-$Cu/Al_2O_3$ |
|---|---|---|---|---|---|---|---|---|
| 250 | 82.3% | 85.5% | 16.6% | 9.2% | 1.2% | 5.3% | 98.8% | 98.3% |
| 275 | 83.6% | 89.1% | 14.4% | 9.9% | 2.0% | 1.0% | 98.8% | 98.4% |
| 300 | 83.1% | 86.2% | 13.5% | 12.9% | 3.5% | 0.8% | 98.7% | 98.7% |
| 325 | 86.0% | 87.4% | 7.5% | 11.9% | 6.5% | 0.7% | 98.7% | 98.8% |

Table 5. Gas feed composition for methane steam reforming at various operating conditions.

| Temperature (°C) | $H_2$ Selectivity $Ni/Al_2O_3$ | $H_2$ Selectivity Ni-$Cu/Al_2O_3$ | $CO_2$ Selectivity $Ni/Al_2O_3$ | $CO_2$ Selectivity Ni-$Cu/Al_2O_3$ | CO Selectivity $Ni/Al_2O_3$ | CO Selectivity Ni-$Cu/Al_2O_3$ | Conversion $Ni/Al_2O_3$ | Conversion Ni-$Cu/Al_2O_3$ |
|---|---|---|---|---|---|---|---|---|
| 500 | 91.2% | 99.1% | 5.8% | 0.7% | 2.9% | 0.3% | 77.0% | 86.3% |
| 550 | 90.2% | 98.1% | 6.8% | 1.1% | 3.1% | 0.8% | 83.6% | 82.7% |
| 600 | 95.3% | 98.8% | 2.1% | 0.8% | 2.6% | 0.4% | 78.2% | 86.2% |
| 650 | 95.4% | 99.0% | 1.4% | 0.6% | 3.2% | 0.3% | 83.9% | 89.2% |
| 700 | 95.7% | 98.8% | 1.3% | 0.8% | 3.0% | 0.4% | 88.9% | 88.7% |

Table 6. Percentage of mass change of commercial and prepared catalysts at various operating conditions.

| Catalyst | % of Mass Change |
|---|---|
| $Cu/ZnO/Al_2O_3$ at 325 °C | 3.2 |
| $Cu/ZnO/Al_2O_3$ at 250 °C | 3.5 |
| $Ni/Al_2O_3$ at 700 °C | 28.3 |
| $Ni/Al_2O_3$ at 500 °C | 16.4 |
| $Ni\text{-}Cu/Al_2O_3$ methane at 700 °C | 2.9 |
| $Ni\text{-}Cu/Al_2O_3$ methane at 500 °C | 3.7 |
| $Ni\text{-}Cu/Al_2O_3$ methanol at 325 °C | 8.3 |
| $Ni\text{-}Cu/Al_2O_3$ methanol at 250 °C | 8.9 |

**Figure 1 (Colour)**
Click here to download high resolution image

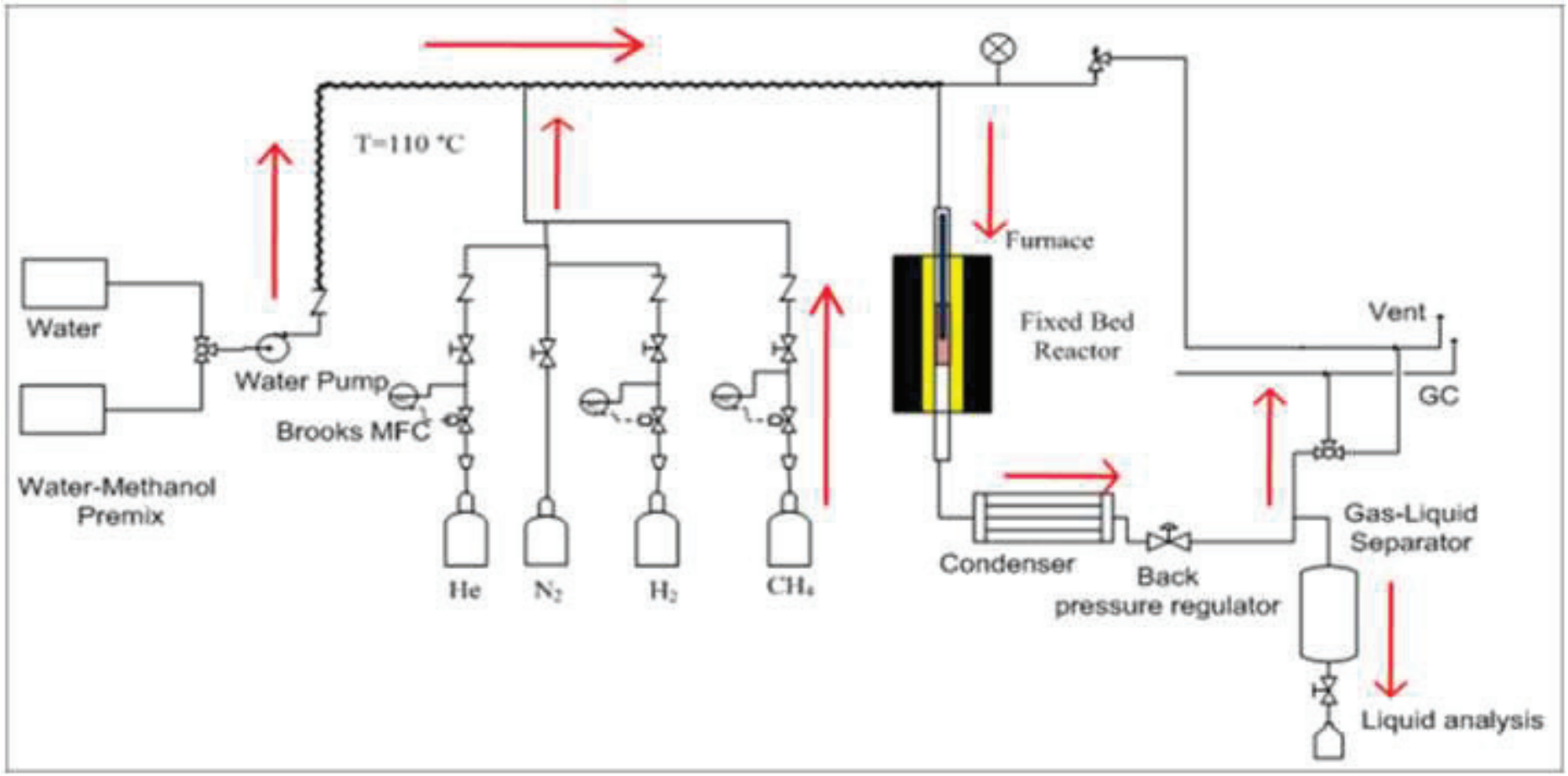

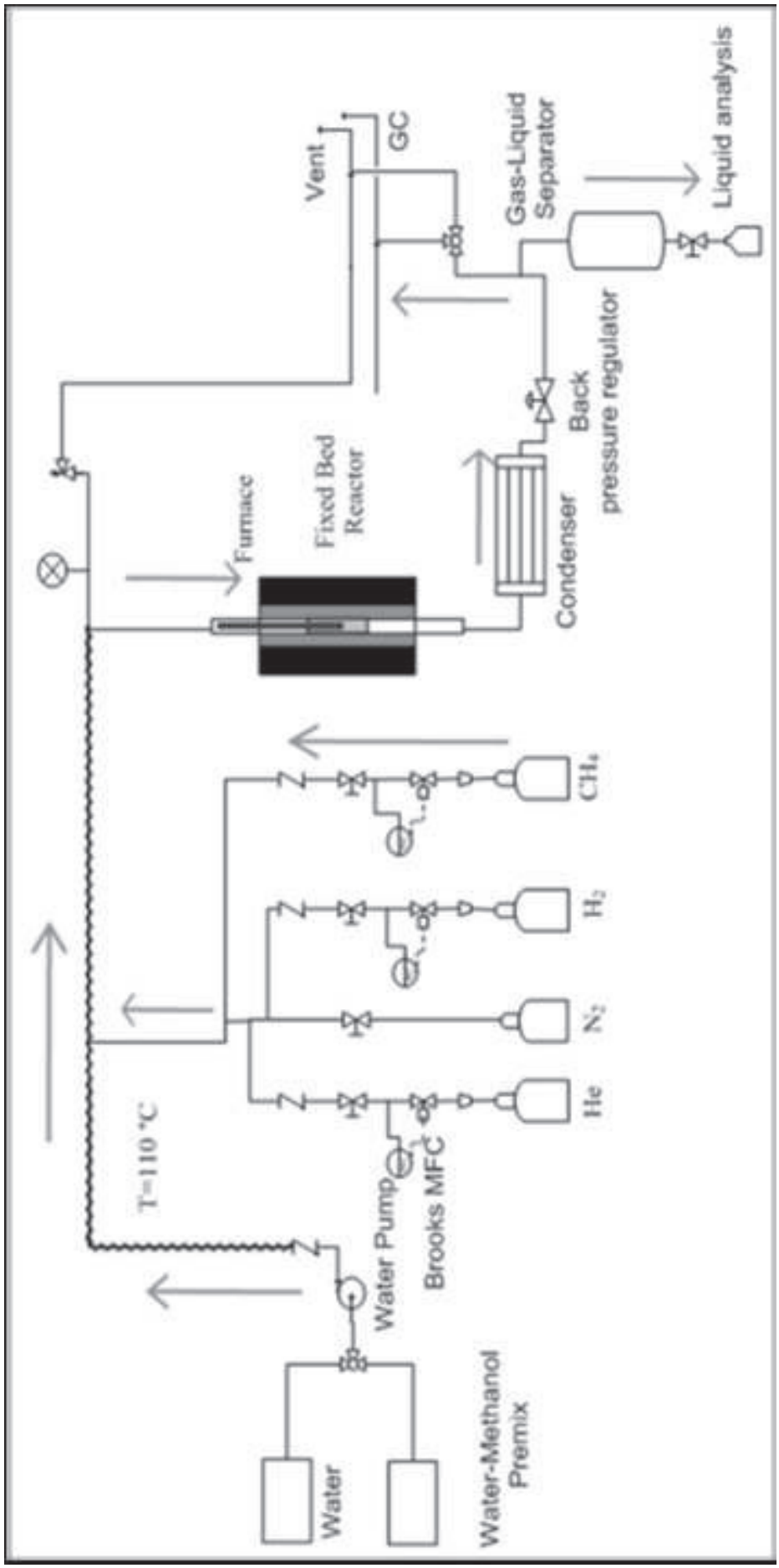


Figure 1 (Black and white)
Click here to download high resolution image

**Figure 2 (Black and white only)**
Click here to download high resolution image

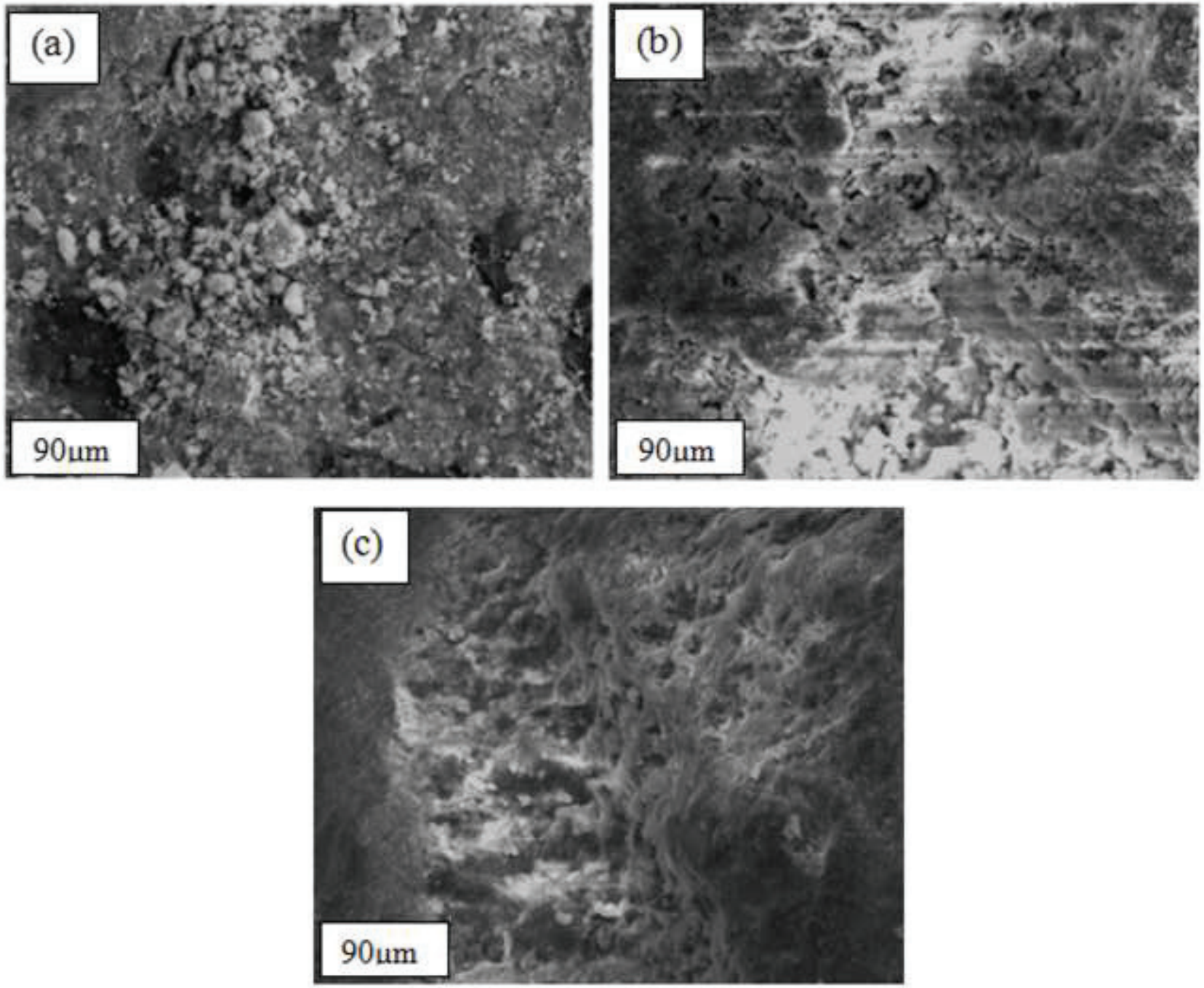

Figure 3 (Colour)
Click here to download high resolution image

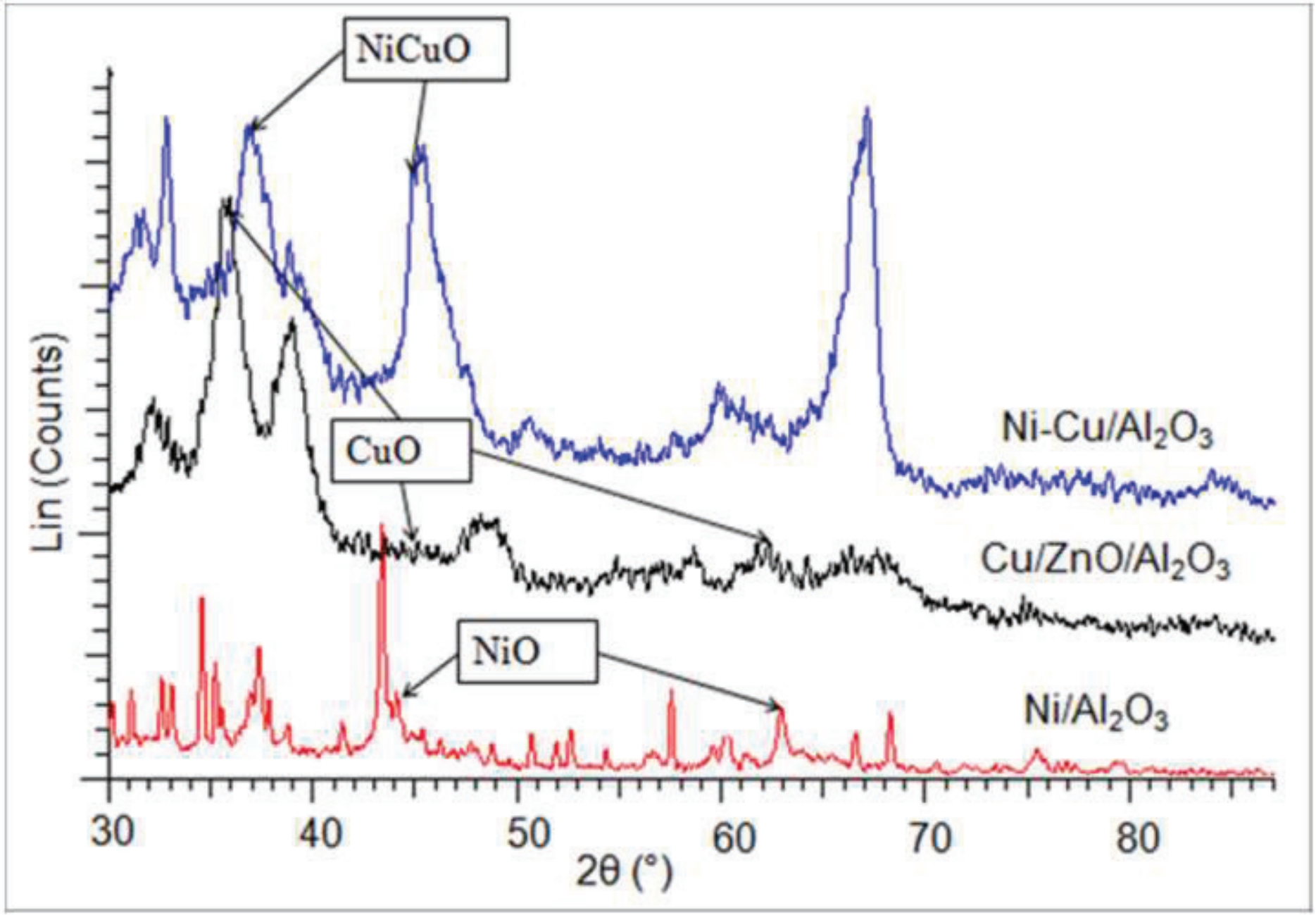

Figure 3 (Black and white)
Click here to download high resolution image

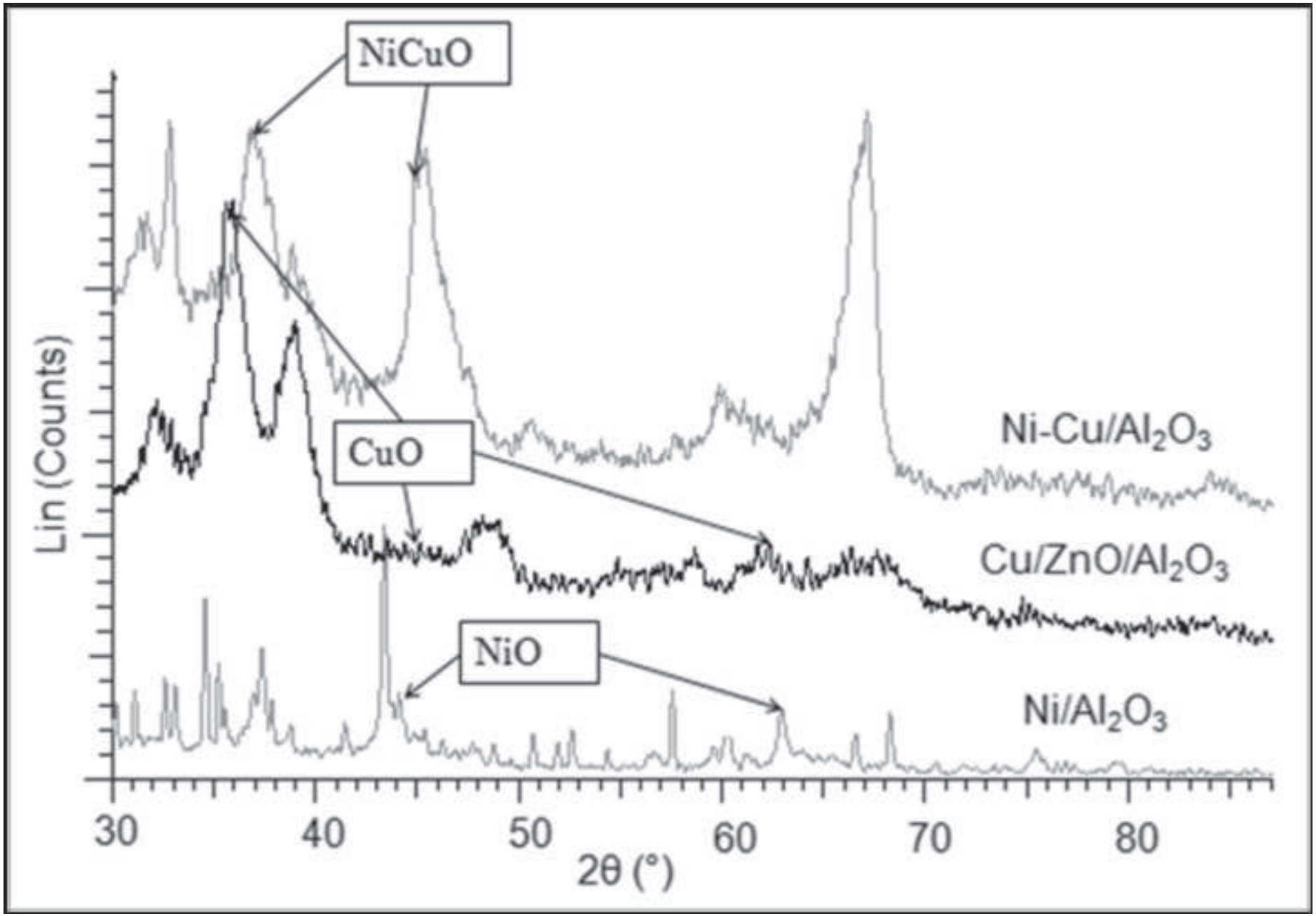

Figure 4 (Colour)
Click here to download high resolution image

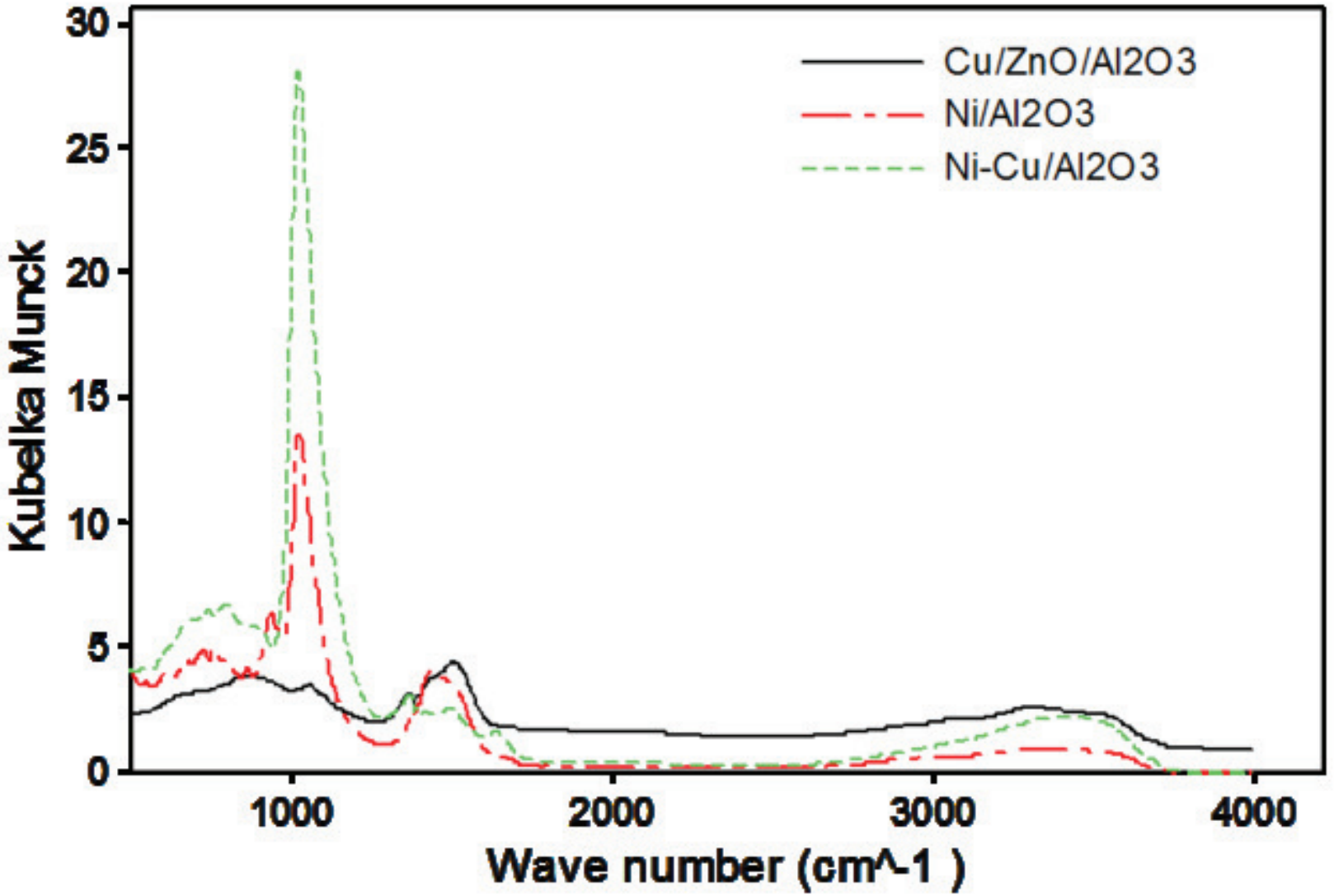

**Figure 4 (Black and white)**
Click here to download high resolution image

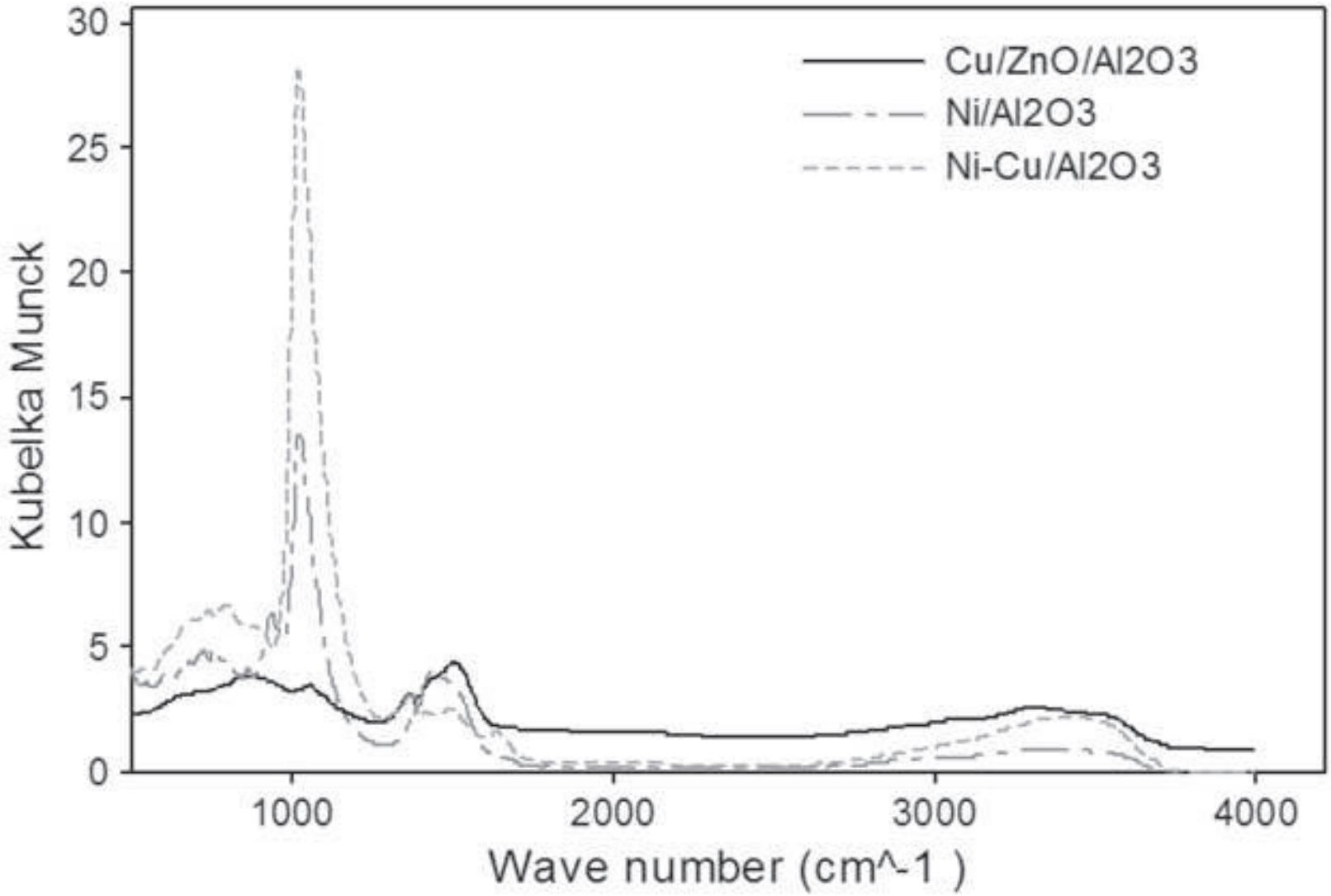

Figure 5 (Colour)
Click here to download high resolution image

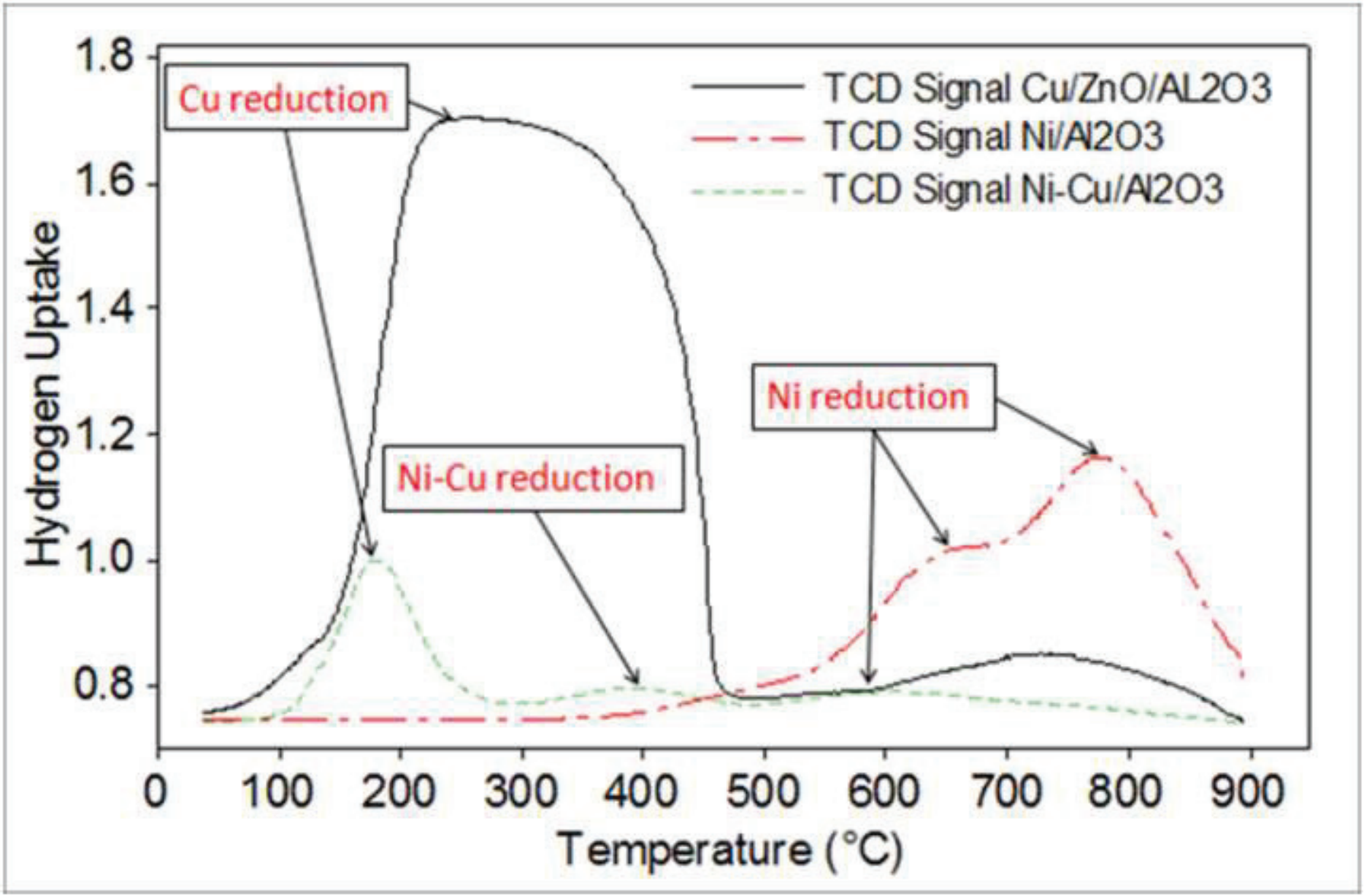

**Figure 5 (Black and white)**
Click here to download high resolution image

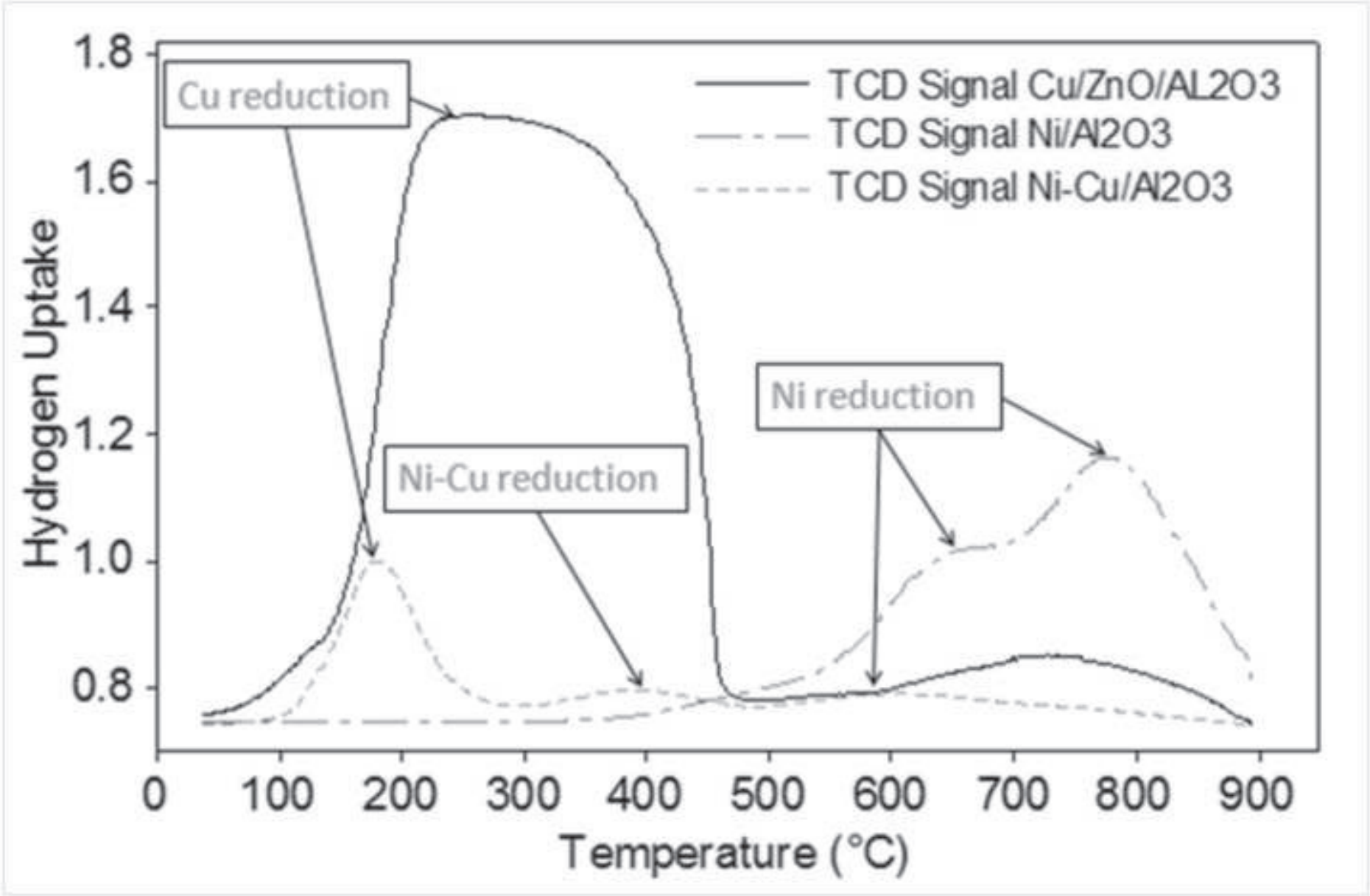

Figure 6 (Colour)
Click here to download high resolution image

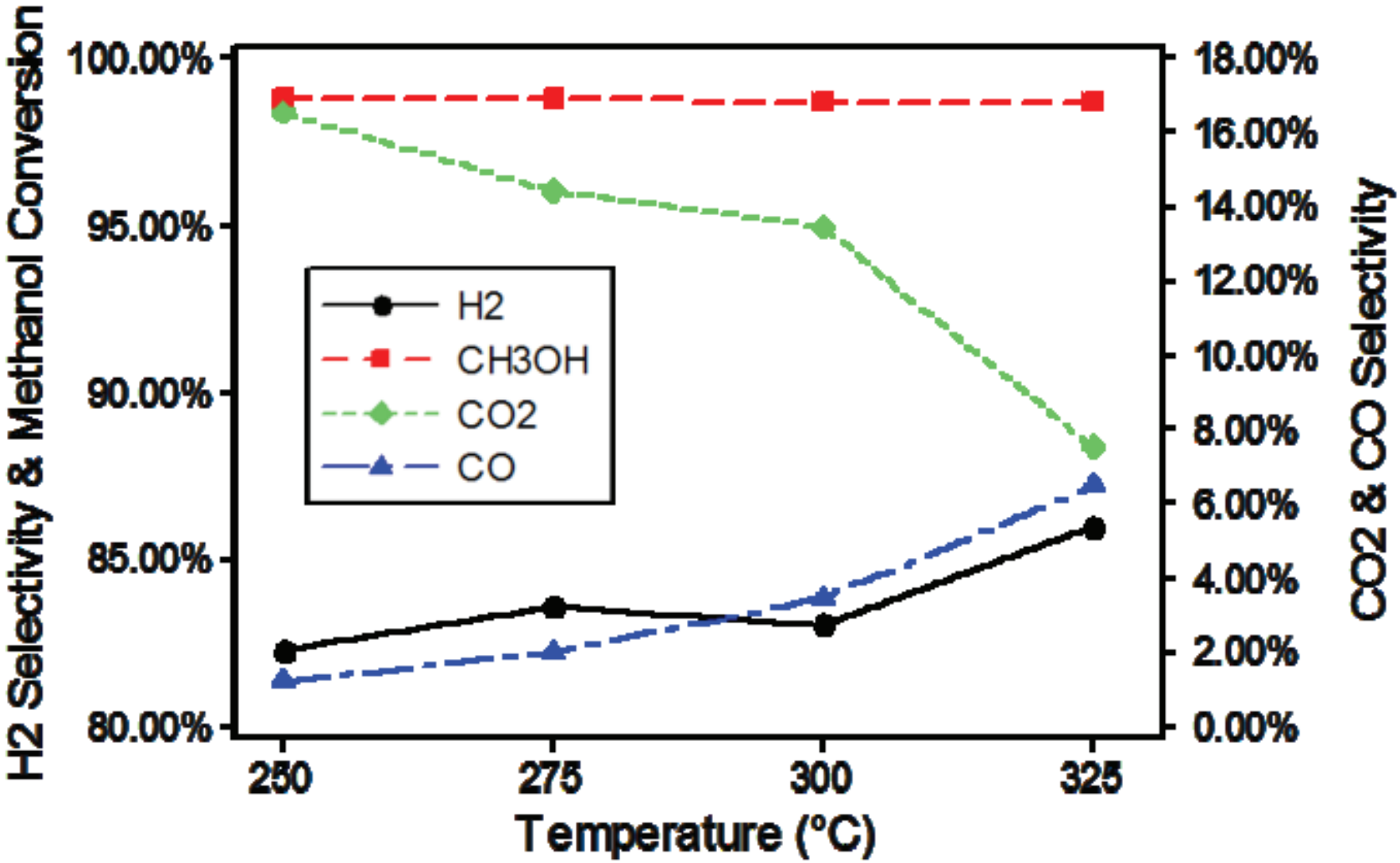

**Figure 6 (Black and white)**
Click here to download high resolution image

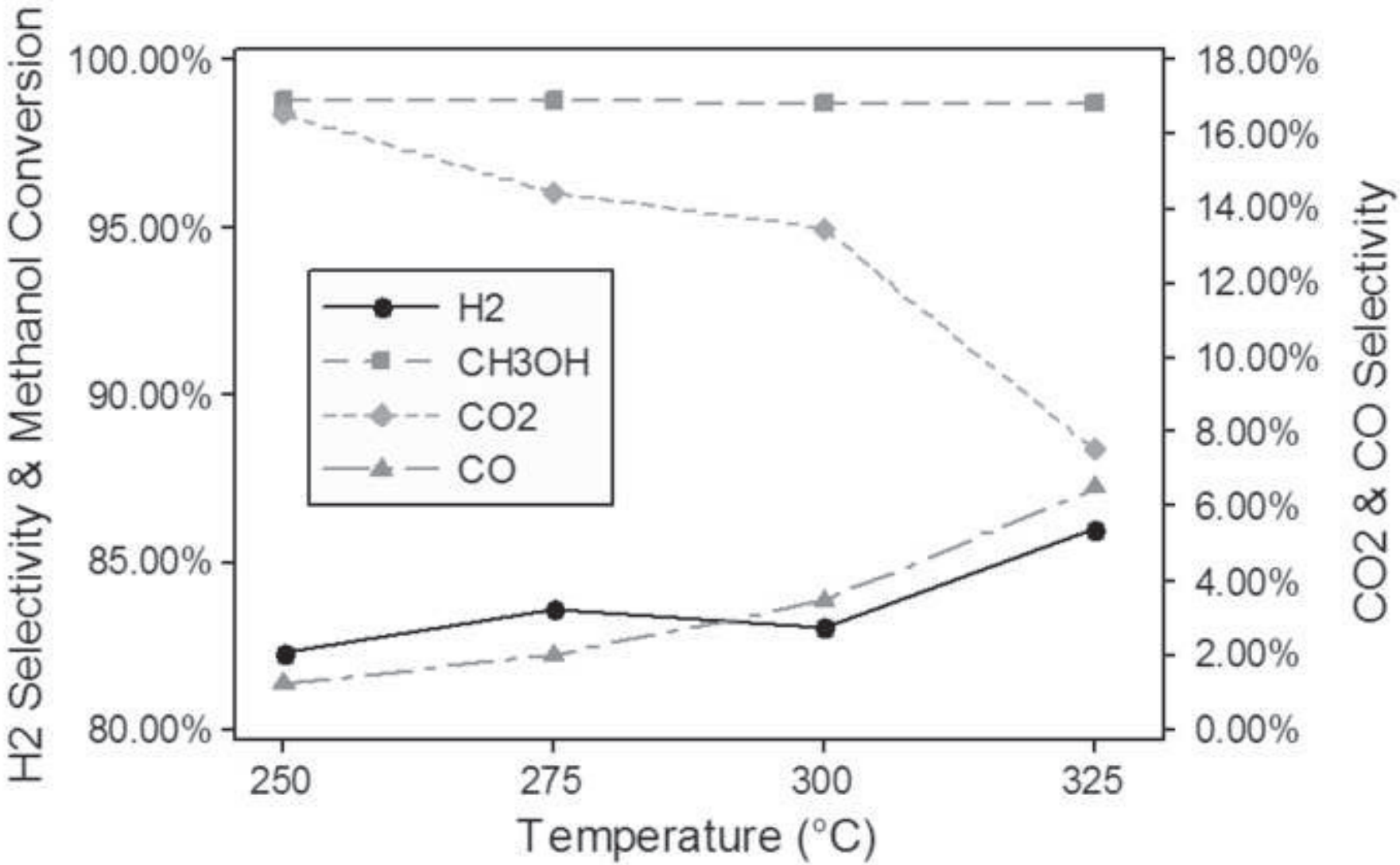

Figure 7 (Colour)
Click here to download high resolution image

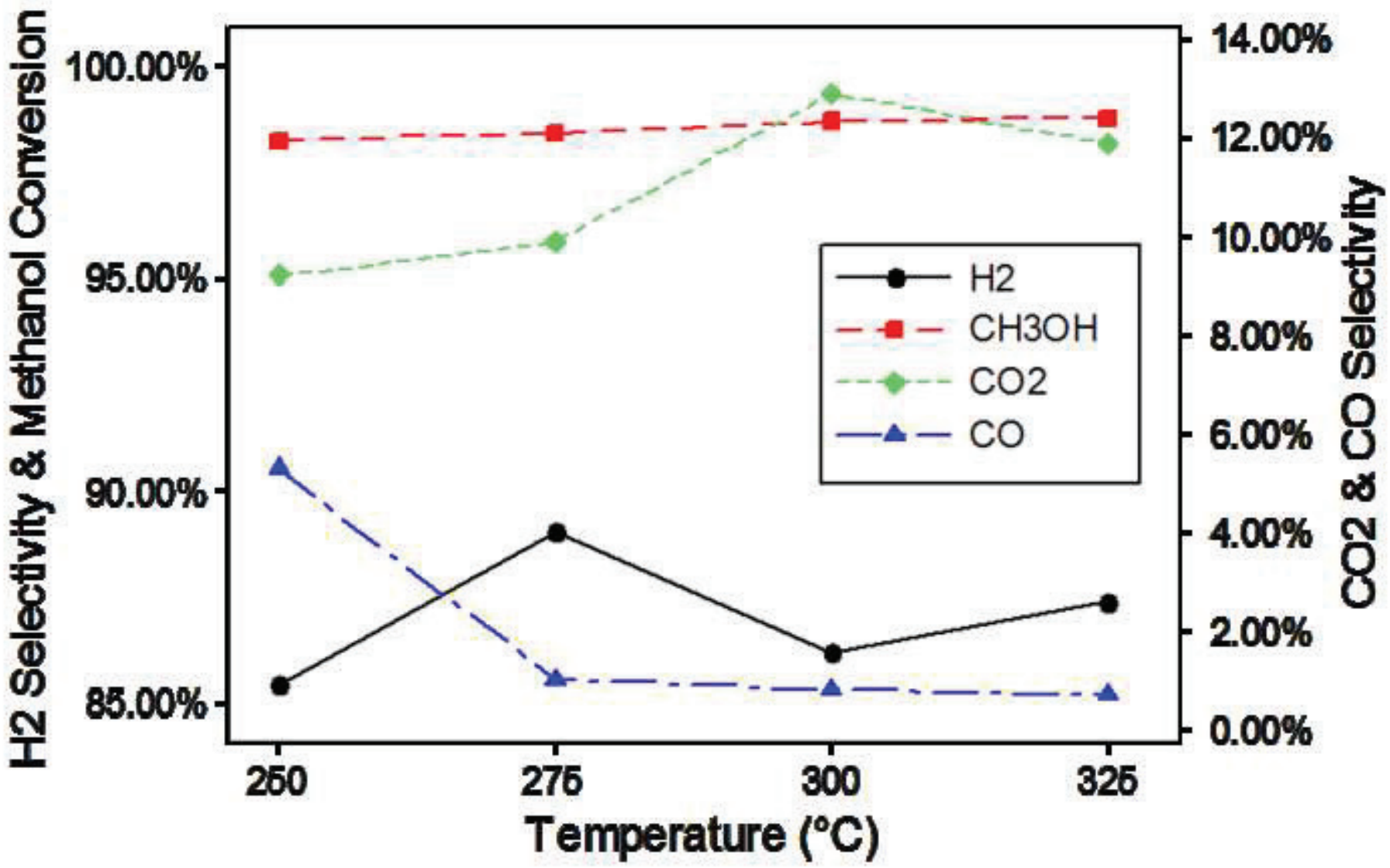

Figure 7 (Black and white)
Click here to download high resolution image

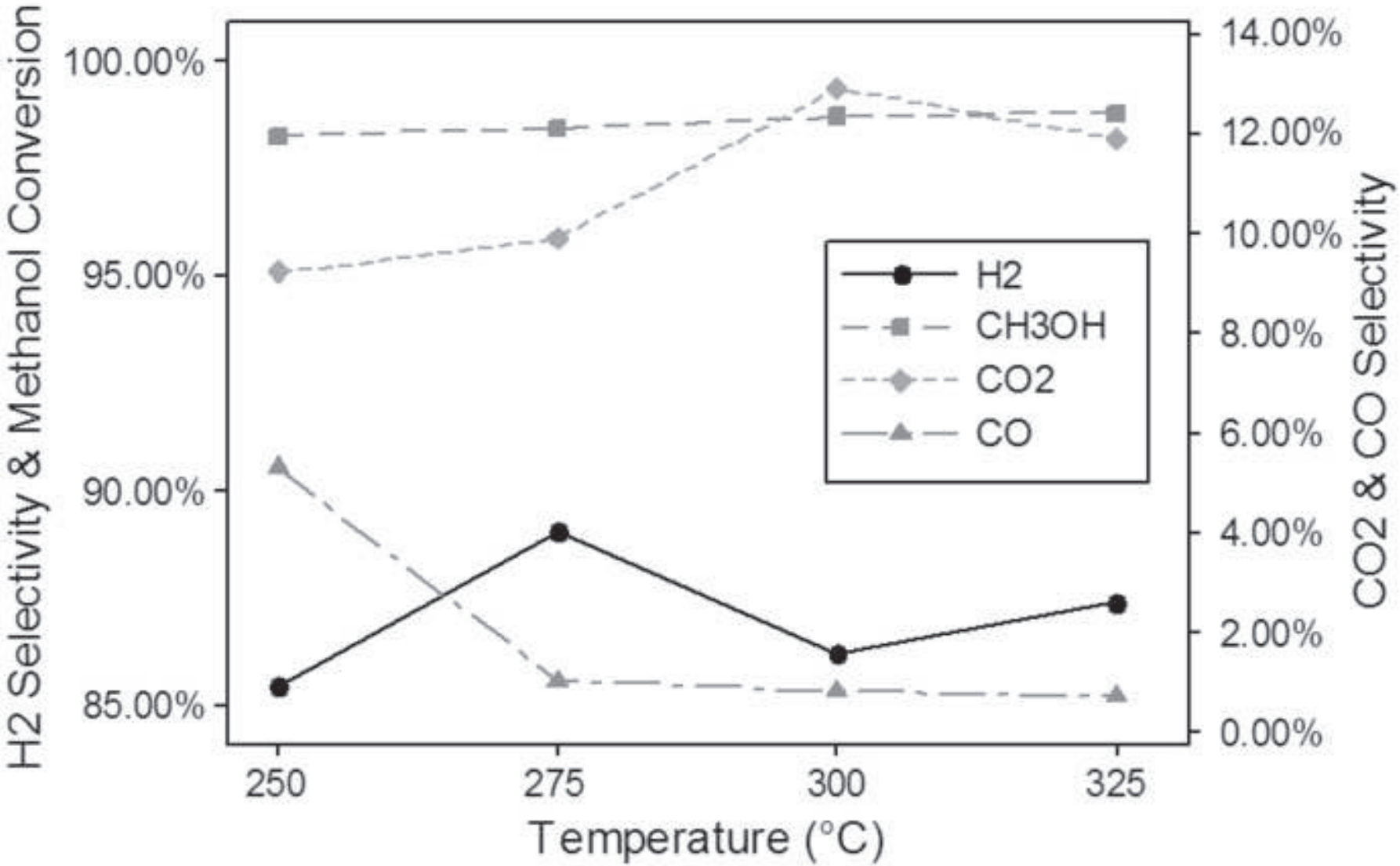

Figure 8 (Colour)
Click here to download high resolution image

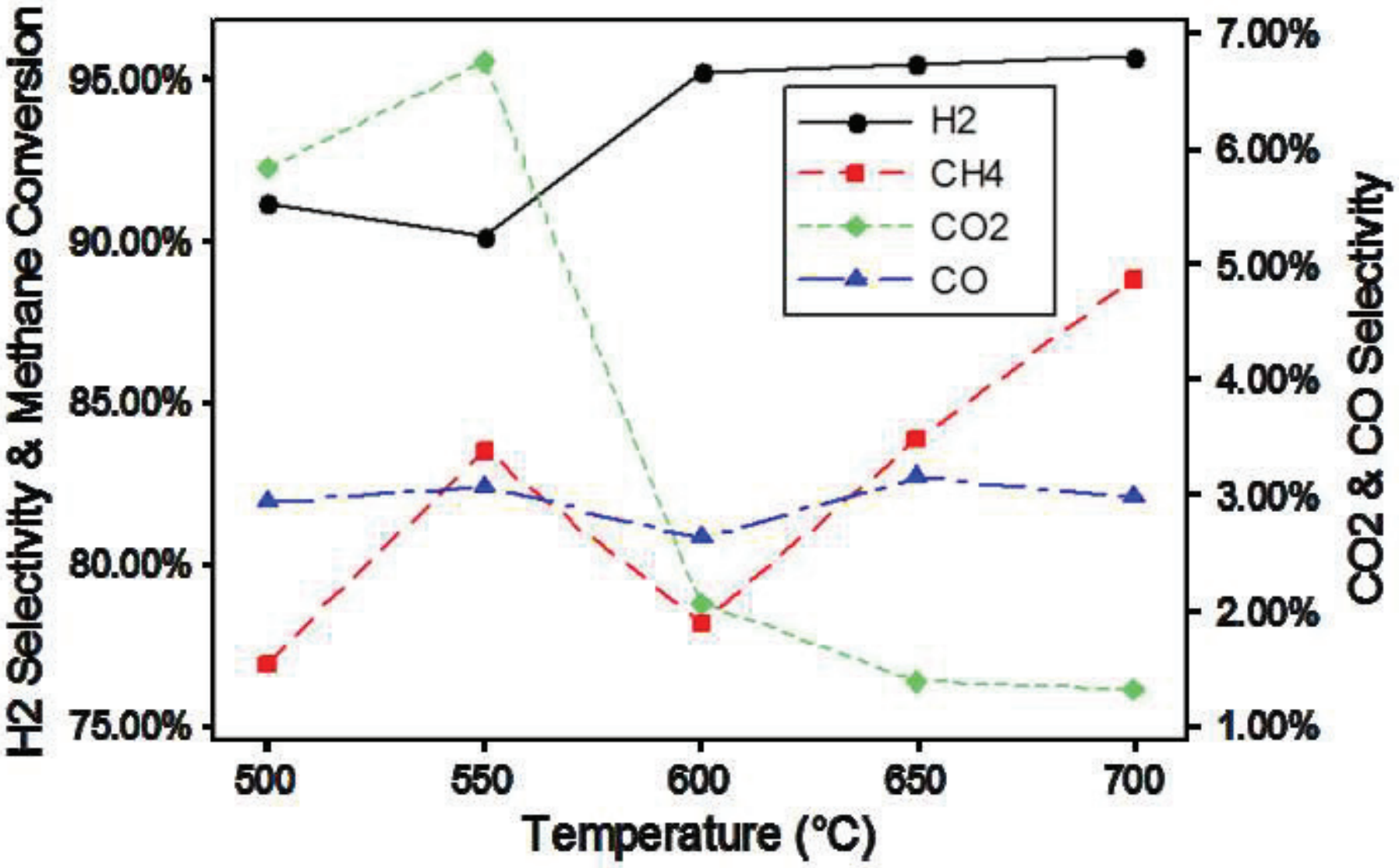

Figure 8 (Black and white)
Click here to download high resolution image

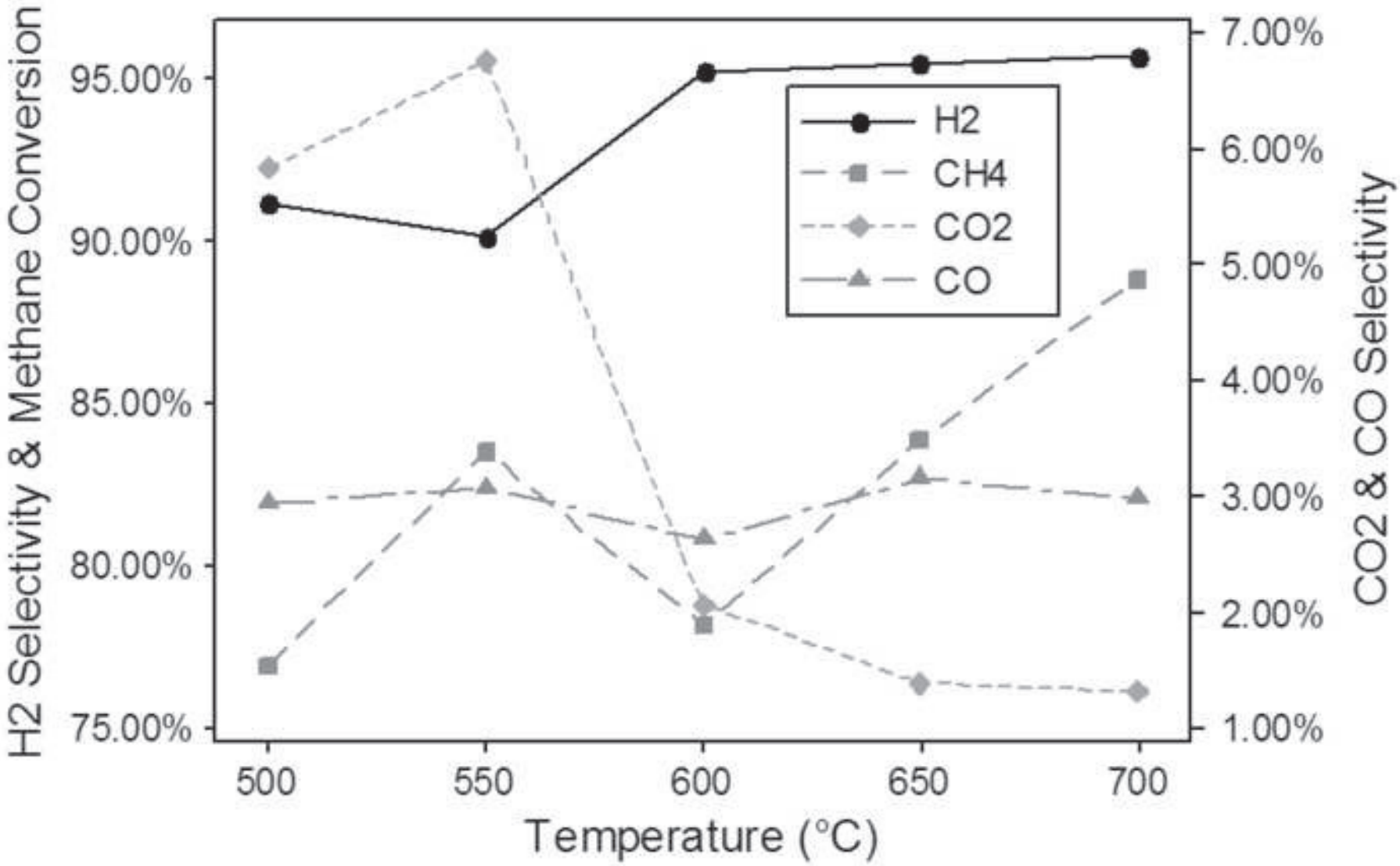

Figure 9 (Colour)
Click here to download high resolution image

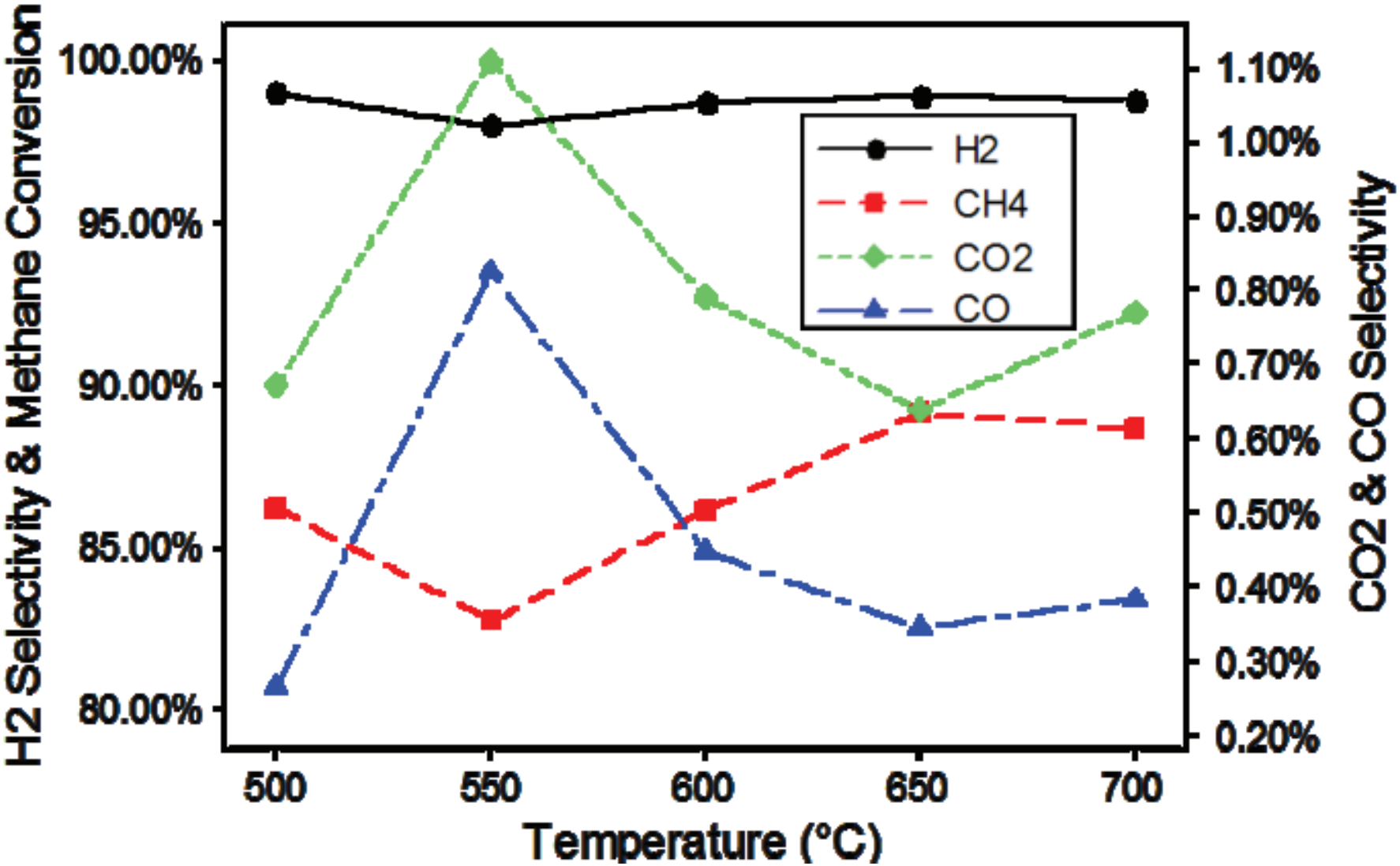

**Figure 9 (Black and white)**
Click here to download high resolution image

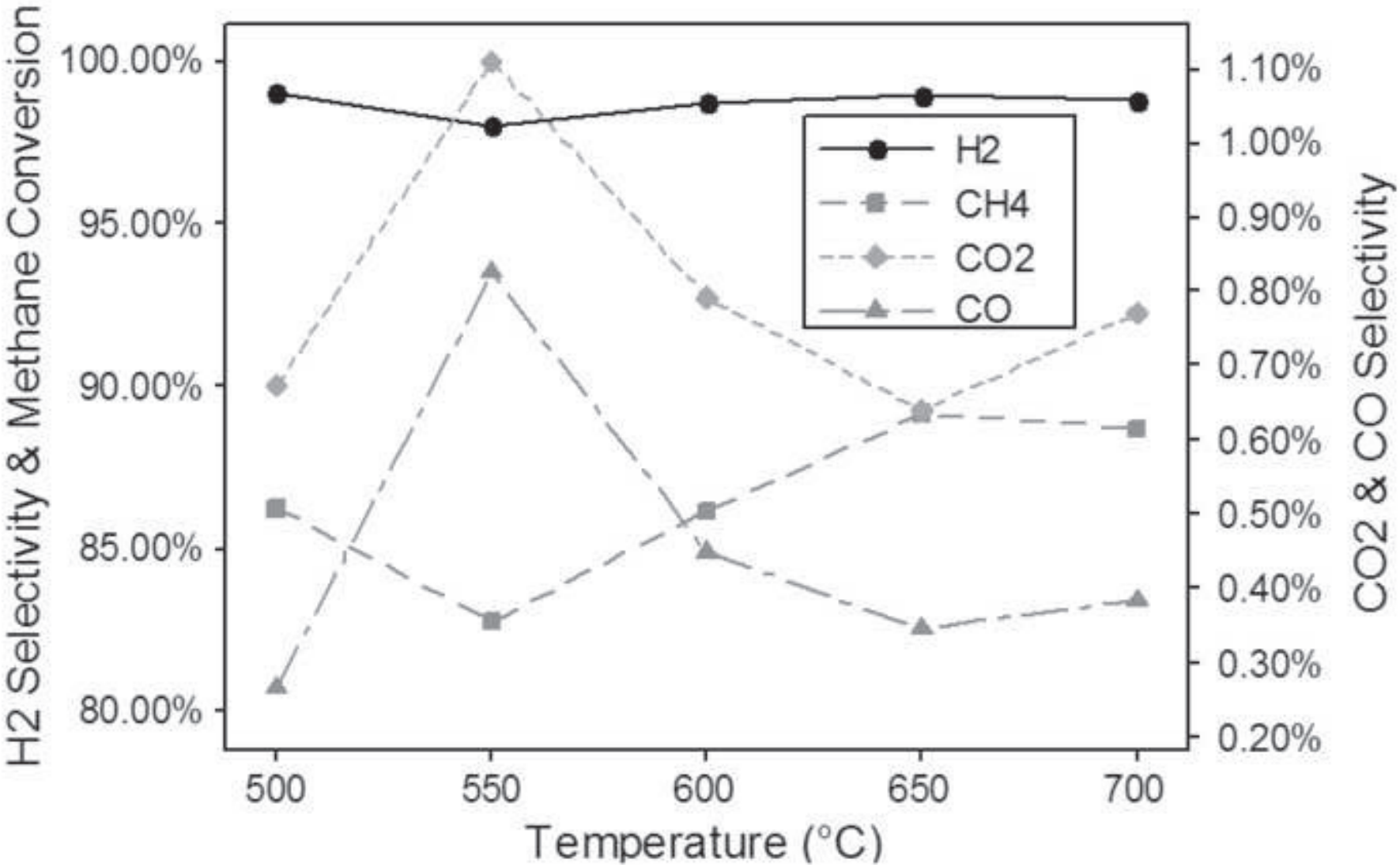

Figure 10 (Black and white only)
Click here to download high resolution image

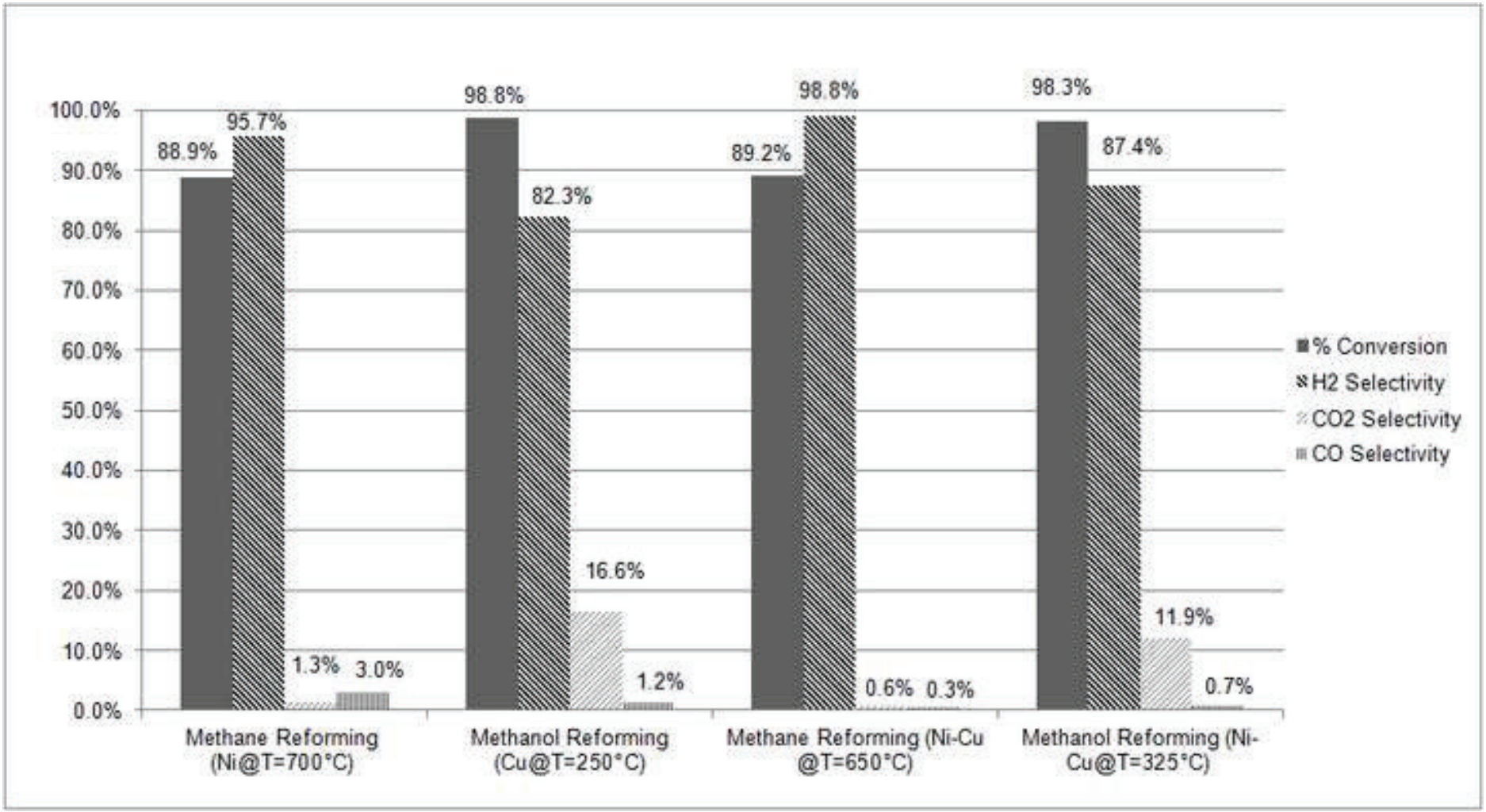

**Figure 11 (Colour)**
Click here to download high resolution image

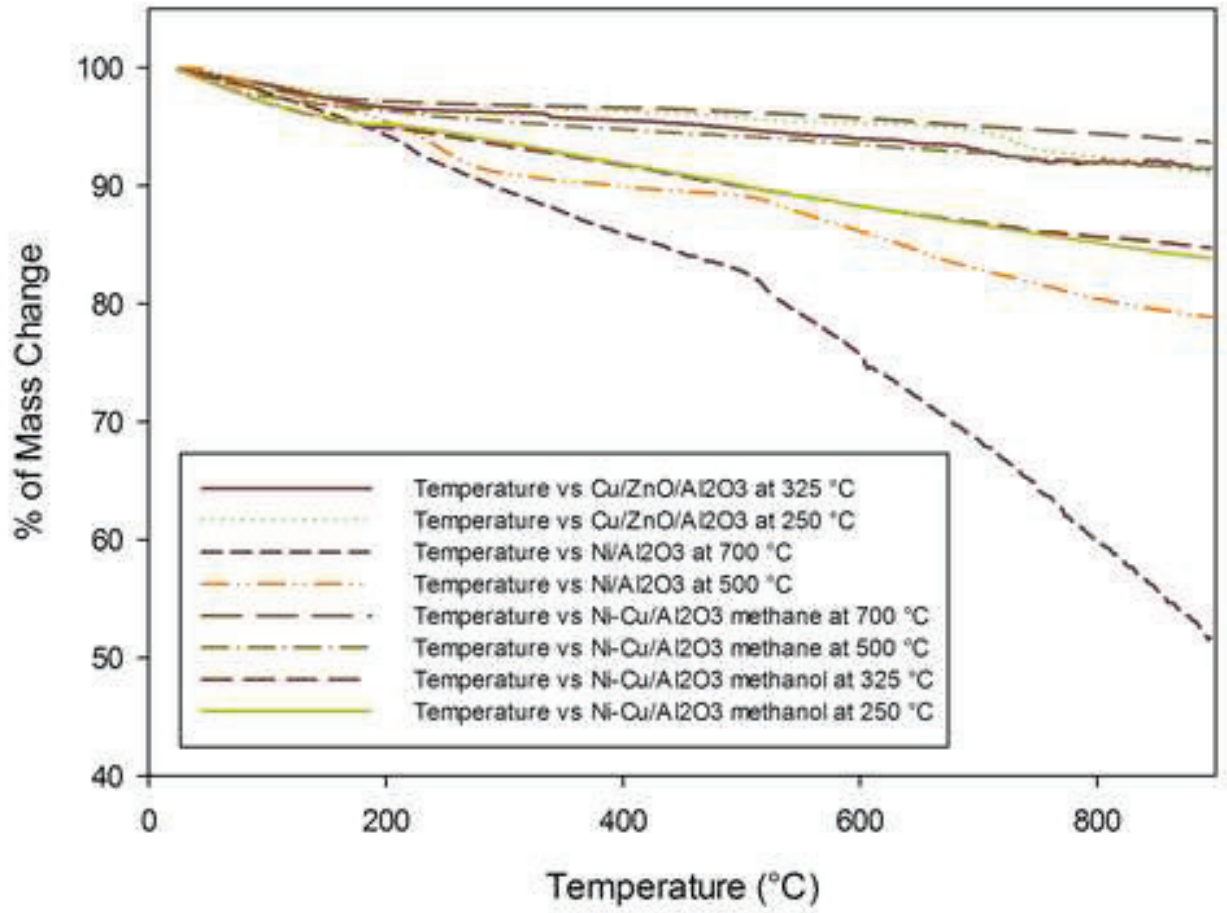

**Figure 11 (Black and white)**
Click here to download high resolution image

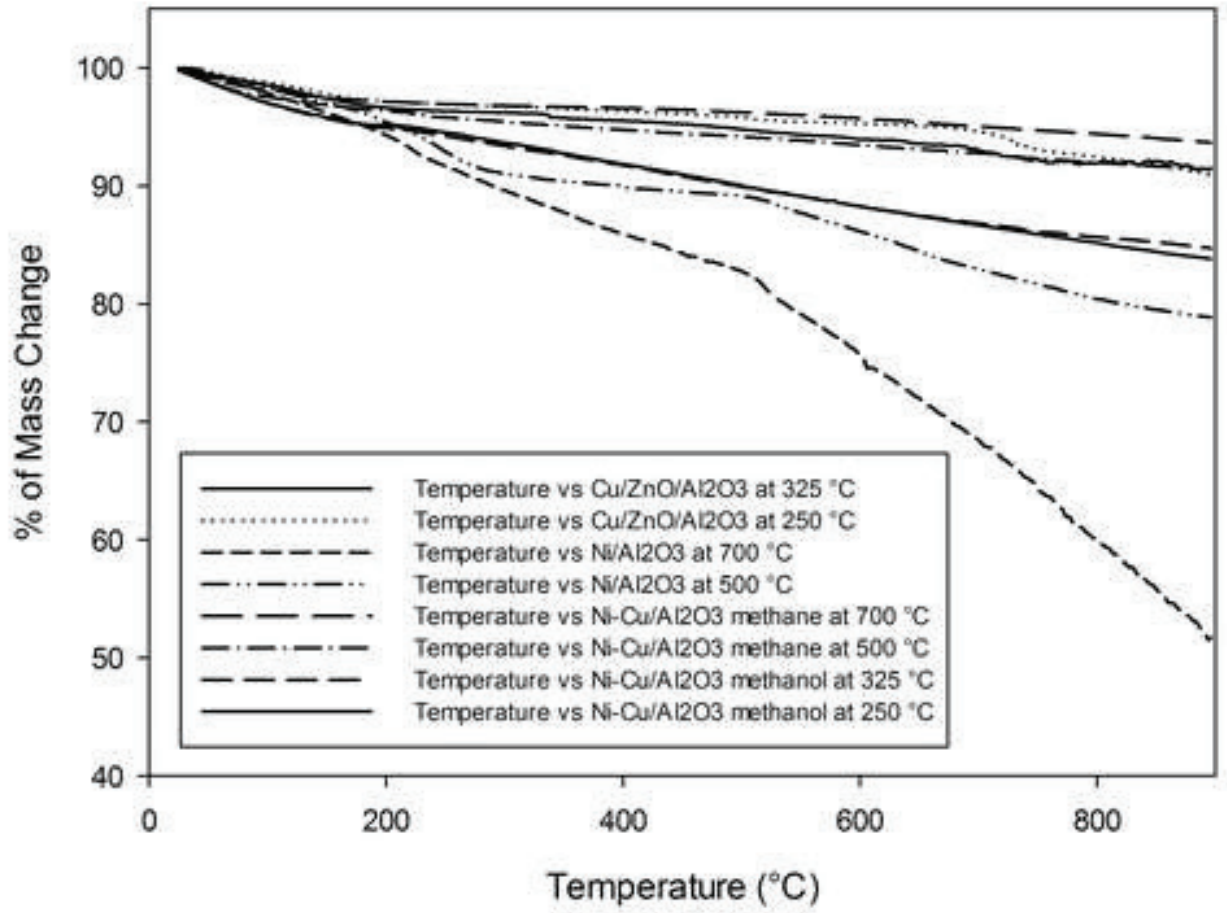

**Supplementary Material**

Click here to download Supplementary Material: Marked Manuscript.docx